PRECAPILLARY OXYGENATION OF PULMONARY ARTERIAL BLOOD

by

Robert Lough Conhaim

B.S. Ed., Ohio State University 1968

DISSERTATION

Submitted in partial satisfaction of the requirements for the degree of

DOCTOR OF PHILOSOPHY

in

PHYSIOLOGY

in the

GRADUATE DIVISION

(San Francisco)

of the

UNIVERSITY OF CALIFORNIA

Approved: Norman C. Staub

Julien I. E. Hoffman

Malcolm B McIlroy

Committee in Charge

Deposited in the Library, San Francisco Medical Center:

Date .... Librarian

Degree Conferred: APR 3 1977

UMI

Dissertation Title:

PRECAPILLARY OXYGENATION OF PULMONARY ARTERIAL BLOOD

Submitted by ROBERT LOUGH CONHAIM in partial satisfaction of the requirements for the degree of Doctor of Philosophy in Physiology, University of California, San Francisco, April, 1977.

ABSTRACT:

The specific issue I have attempted to answer, both experimentally and theoretically, is whether any significant quantity of oxygen enters the pulmonary blood before it reaches the alveolar wall capillaries. The pulmonary arteries, especially the smaller ones, are surrounded by alveolar gas at relatively high oxygen tension, and the walls of all pulmonary arteries are thin relative to systemic arteries of equivalent diameter. Therefore it is possible that oxygen diffuses across the walls of pulmonary arteries to oxygenate, at least partially, the blood that is flowing through them.

On a more general level, the local regulation of vascular resistance as well as the diffusion of oxygen into aerobically respiring systemic tissue could involve gaseous exchange through the walls of precapillary vessels. Although that issue is not directly involved in my thesis research, it is an area of potential investigation by the methods I have developed here.

With the aid of several experts I built a spectrophotometer as part of a microscope system that allowed me to record oxyhemoglobin saturation values with the light reflected from transected, frozen pulmonary arteries. It measures from an area 100 μm in diameter, and does so with an accuracy of plus or minus 5%. I prepared anesthetized cats to provide optimum conditions for precapillary oxygenation, quickly froze their lungs with chilled liquid propane, and removed them. Cross sections of these lungs were examined with the microspectrophotometer, and data indicating the presence of precapillary oxygenation were recorded.

While propane freezes lungs quickly it does not capture the conditions present there exactly as they are in life. The cat experiments revealed that precapillary oxygenation may occur under the right circumstances, but they did not tell me how much this process normally contributes to total lung oxygenation. I attempted to answer this question by making several calculations with available data on pulmonary arterial geometry and diffusing capacity.

I concluded that a significant fraction of the total oxygenation of pulmonary arterial blood may occur before that blood reaches the alveolar capillaries. As much as 15% may be oxygenated by this process at rest, and when breathing pure oxygen as much as 100%. This process could be of considerable importance in special circumstances when pulmonary arterial blood flow through large vessels is slowed. Emphysematous patients often have large air spaces within their lungs that are traversed by relatively large vessels. Blood flow through such vessels is slow, and transvascular oxygen flux may make an important contribution to the oxygenation of blood within them.

Approved by: Norman C. Staub

Norman C. Staub M.D., Professor of Physiology
Chairman, Dissertation Committee

UMI

ACKNOWLEDGEMENT

Though only my name appears on the title page of this dissertation, several people are responsible for the successful completion of the work described here.

I wish especially to thank Professor Norman C. Staub for his patient and critical advice during my tenure as a graduate student in his laboratory, and also to thank Professors Julien I. E. Hoffman and Malcolm B. McIlroy for their guidance in the course of this work and for critically reading the draft of this dissertation.

I would like to thank Gus Winston and Marshal Fong for designing and building the power supply and processing circuitry of the microspectrophotometer, and Jim Wall for manufacturing many of its component parts.

Betty Dornbusch and the staff of the Cardiovascular Research Institute's Physiological Services Laboratory were very kind to interrupt their busy schedules to complete the analyses of the numerous blood samples I brought to them.

Thanks, too, to Oscar Osorio for his technical assistance with the animal preparations.

UMI

FINANCIAL ASSISTANCE

During my research work I was supported by a Training Grant from the National Institute of Health (USPHS GM-00927), a Graduate Training Grant from the National Heart, Lung, and Blood Institute (HLO-5251), and an award from the Earl C. Anthony Trust for Graduate Student Research.

TABLE OF CONTENTS

Chapter 1 Introduction 1

Chapter 2 History 3

Anatomical and Physiological Evidence for Transvascular Oxygen Flux 3

Spectrophotometry of Hemoglobin 7

Bulk Oxygenation of Blood 14

Chapter 3 Microspectrophotometry 17

Description 17

Tests 23

Operating Practices 44

Discussion 47

Chapter 4 Cat Experiments 53

Isolated-Perfused Cat Lungs 53

Precapillary Oxygenation (100% Oxygen) 57

Freezing Time 65

Clamped Hilum 67

Precapillary Oxygenation (Air) 69

Discussion 71

Chapter 5 Models 74

Calculation of Rim Thickness 74

Polyethylene Tube Experiments 80

Discussion 83

Chapter 6 Discussion and Conclusions 85

REFERENCES 94

UMI

Chapter 1 INTRODUCTION

The specific issue I have attempted to answer, both experimentally and theoretically, is whether any significant quantity of oxygen enters the pulmonary blood before it reaches the alveolar wall capillaries. The pulmonary arteries, especially the smaller ones, are surrounded by alveolar gas at relatively high oxygen tension, and the walls of all pulmonary arteries are thin relative to systemic arteries of equivalent diameter. Therefore it is possible that oxygen diffuses across the walls of pulmonary arteries to oxygenate, at least partially, the blood that is flowing through them.

On a more general level, the local regulation of vascular resistance as well as the diffusion of oxygen into aerobically respiring systemic tissue could involve gaseous exchange through the walls of precapillary vessels. Although that issue is not directly involved in my thesis research, it is an area of potential investigation by the methods I have developed here.

With the aid of several experts I built a spectrophotometer as part of a microscope system that allowed me to record oxyhemoglobin saturation values with the light reflected from transected, frozen pulmonary arteries. It measures from an area 100 μm in diameter, and does so with an accuracy of plus or minus 5%. I prepared anesthetized cats to provide optimum conditions for precapillary oxygenation, quickly froze their lungs with chilled liquid propane, and removed them. Cross sections of these lungs were examined with the microspectrophotometer, and data indicating the presence of precapillary oxygenation were recorded.

While propane freezes lungs quickly (36), it does not capture the conditions present there exactly as they are in life. The cat experiments revealed that precapillary oxygenation may occur under the right circumstances, but they did not tell me how much this process normally contributes to total lung oxygenation. I attempted to answer this question by making several calculations with available data on pulmonary arterial geometry and diffusing capacity.

I concluded that a significant fraction of the total oxygenation of pulmonary arterial blood may occur before that blood reaches the alveolar capillaries. As much as 15% may be oxygenated by this process at rest, and when breathing pure oxygen as much as 100%. This process could be of considerable importance in special circumstances when pulmonary arterial blood flow through large vessels is slowed. Emphysematous patients often have large air spaces within their lungs that are traversed by relatively large vessels. Blood flow through such vessels is slow, and transvascular oxygen flux may make an important contribution to the oxygenation of blood within them.

UMI

Chapter 2 HISTORY

ANATOMICAL AND PHYSIOLOGICAL EVIDENCE FOR TRANSVASCULAR OXYGEN FLUX

The vessels carrying blood to the pulmonary capillaries are embedded in the lung's gas-filled alveolar parenchyma. It seems reasonable that under favorable conditions oxygen should diffuse from the alveoli, through the walls of these vessels, and into the mixed venous blood flowing through them (Fig. 2-1). Gas exchange therefore need not be confined to the pulmonary capillaries. "Favorable conditions" include: a vessel wall that is sufficiently permeable to oxygen; a sufficient gradient for diffusion from the gas compartment to the precapillary blood; and most importantly, a sufficient time spent by the blood flowing in these vessels for exchange to occur before the blood reaches the alveolar capillaries.

The structure of pulmonary arteries is especially conducive to this phenomenon for they have thinner walls than systemic arteries of equivalent diameter. Hayek (14) has pointed out that pulmonary arteries with diameters of 6 mm have only 10 circular muscle layers, with this number decreasing to 6 in vessels of 2 mm, and to 1 or 2 in vessels between 0.1 and 0.15 mm. Further, their elasticae intimae are discontinuous, and their adventitiae only weakly developed compared to that in systemic arteries. Figure 2-1 shows 2 magnifications of a cat

UMI

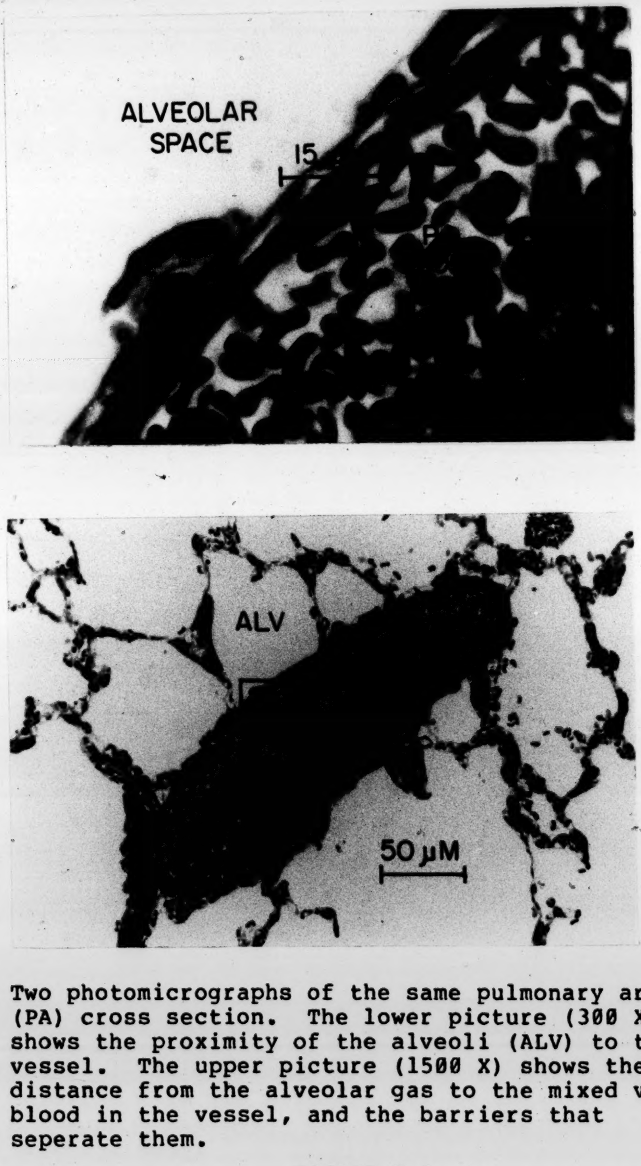

Two photomicrographs of the same pulmonary artery (PA) cross section. The lower picture (300 X) shows the proximity of the alveoli (ALV) to the vessel. The upper picture (1500 X) shows the distance from the alveolar gas to the mixed venous blood in the vessel, and the barriers that seperate them.

FIGURE 2-1

UMI

pulmonary artery 75 um in diameter. The structural features of the vascular wall are clearly visible in the upper picture. The most important feature of the figure is that it clearly shows that the diffusion distance for oxygen is only about 5 μm from the alveolar space to the mixed venous, pulmonary arterial blood in this vessel. As the caliber of pulmonary arteries decreases in successive generations, the walls become as thin as 1.5 μm in vessels with diameters of 15 μm, and the surface area-to-volume ratio increases proportionally.

In recent years several pieces of evidence have accumulated to support this idea. In 1961, Staub (33) reported that he observed bright red oxygenated blood in small pulmonary arterioles (100-200 μm diam.) of whole frozen cat lungs that had been ventilated with 100% oxygen before death. Jameson (15) placed platinum tipped cardiac catheters sensitive to oxygen and hydrogen into pulmonary arteries of 27 patients undergoing right heart catheterization. In 16 patients oxygen was detected in less that 1.0 sec. His catheter was 2.5 mm in diameter and placed in the wedged position or 1-3 cm proximal to it. In the same year, Sobol, et al (32) did similar experiments in 34 patients with hydrogen and a catheter 1.5 mm in diameter. The response times averaged 1.9 sec. with the catheter wedged. Munson, et al (22,23) reported that patients suffering from venous air embolism during surgery experienced a rise in pulmonary arterial pressure after their anesthetic gas was changed from halothane to nitrous oxide. He

UMI

concluded that nitrous oxide diffused from the alveoli through the walls of the embolized pulmonary arteries and into the embolus itself causing it to expand and further occlude the vessel. This produced the rise in pulmonary arterial pressure.

This evidence indicates that gas can diffuse from the alveolar space into the precapillary vessels, but it does not indicate how much this process is likely to occur under normal physiological conditions.

In 1964, Sackner, et al (29) published estimated values for the oxygen diffusing capacities of pulmonary arterioles with diameters as small as 14 µm. They used ether plethysmography to measure the diffusing capacities in arteries as small as 0.3 mm and used anatomical data to extrapolate the values for the smaller vessels. Their technique was crude but these values are the only ones known for the diffusing capacities of these vessels.

The essential information required to calculate the amount of oxygenation that might occur by this process normally is the time the mixed venous blood spends in the pulmonary arterial system before arriving at the alveolar capillaries. The total transit time from the main PA to the capillaries is less than 1.5 sec. in dogs (10,29). The relationship between the diffusing capacities of the vessel walls and the total transit time has to be favorable for the amount of precapillary oxygenation to be significant. An additional important contribution of the paper of Sackner, et al was their estimated values

UMI

for the transit time for blood flow through pulmonary arteries of discrete diameters. When combined with their diffusing capacity data, a prediction of the expected amount of precapillary oxygenation can be made. Sackner, et al claim to have made these calculations though they are not included in their report. They predicted that no significant precapillary oxygenation could occur, even while breathing 100% oxygen.

These conclusions are puzzling in light of the findings of Duling and Berne (8) who used microelectrodes to measure oxygen tensions on the external surfaces of small arterioles in the hamster cheek pouch. When the animals were ventilated with 95% oxygen, the partial pressure of oxygen fell from 150 torr on the surface of 80 μm arterioles to 40 torr on the surface of the terminal arterioles. They concluded that there was a considerable oxygen loss from the blood as it flowed through these vessels. Systemic arterioles have thicker and more muscular walls than their pulmonary counterparts; this makes Sackner's conclusions especially hard to understand.

SPECTROPHOTOMETRY OF HEMOGLOBIN

Introduction

In 1961, Staub (33) reported that he had observed bright red oxygenated blood in the precapillary vessels of whole frozen cat lungs. One year later, he and Storey (36) reported that rapid freezing was a

UMI

useful method for relating morphological and physiological events in the lung because it provided the capability of capturing and maintaining blood in the state of oxygenation at which it existed at the time of freezing. These developments meant that I could apply previously developed techniques of spectrophotometry directly to this frozen blood. This allowed me to measure intravascular oxyhemoglobin saturations *in situ* in pulmonary arteries and arterioles.

General Considerations

Four things can happen to light when it illuminates an absorbing medium such as hemoglobin: it can be reflected; refracted; pass completely through; or it can be absorbed and re-emitted as heat or light (fluorescence or phosphorescence). The predominant effect depends on the nature of the pigment and the wavelength of the incident light.

The Lambert-Beer Law of absorption describes the attenuation of the incident light as it traverses the absorbing medium. A wavelength of incident light is chosen such that the light will be absorbed strongly by the pigment. A solution of pigment is placed in an optical-glass chamber with a known light path length and the attenuation of the light after it passes through the pigment is measured. If the concentration of the pigment solution is one molar,

UMI

and if the light passes through a column of pigment one cm. long, the degree to which the incident light is diminished is called the "molar extinction coefficient" and is numerically equal to the log(10) of the ratio of the intensity of the incident light to the intensity of the transmitted light. If the concentration of the pigment, or the path length are different from these standard values, the log(10) ratio of the intensities is known as the "optical density" (O.D.). This can be state mathematically as:

$$\text{O.D.} = \log_{10} \frac{I_o}{I} = E\ c\ L$$

where:

E = molar extinction coefficient
c = conc. of pigment solution (moles/liter)
L = optical path length of light (cm)
I = intensity of incident light
I_o = intensity of transmitted light

Hemoglobin in equilibrium with oxygen actually results in two pigments - hemoglobin and oxyhemoglobin. Each of these has its own unique wavelengths of absorption (Fig. 2-2). This quality allows the relative concentrations of the two to be determined by making absorption measurements at two different wavelengths. One is made at a wavelength where hemoglobin and oxyhemoglobin absorb equally. In Figure 2-2 these "isosbestic points" occur for example at 580 and 810

ABSORPTION SPECTRA OF

HEMOGLOBIN AND OXYHEMOGLOBIN

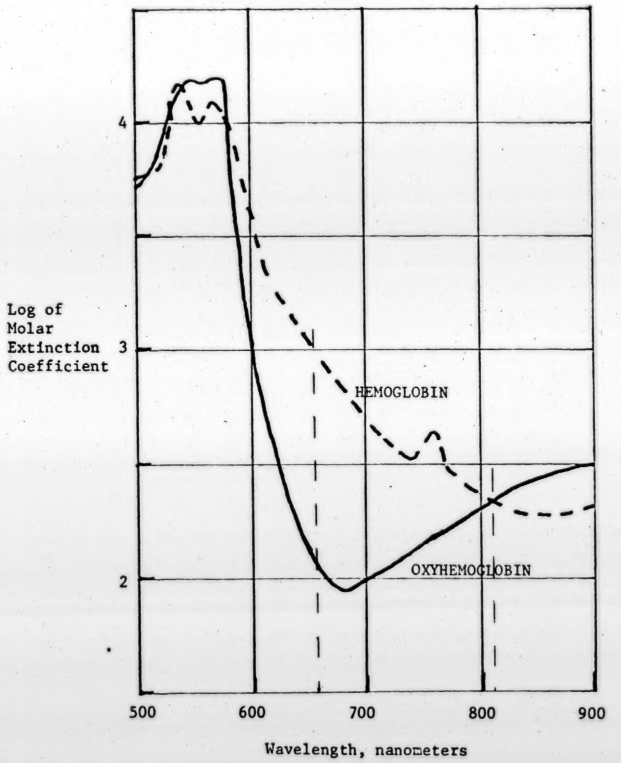

Redrawn from Gordy and Drabkin(12)

FIGURE 2-2

UMI

nm. A measurement is also made at a wavelength where the spectra are different, at 660 nm for example. The first wavelength provides a measure of the overall hemoglobin concentration of the solution, while the second measures the relative concentration of oxyhemoglobin in it. The ratio of the optical densities at the two wavelengths is an expression of the oxygen saturation of the solution.

Theoretically, any combination of isosbestic point and differential wavelength should be suitable, though in practice a pair should be chosen that are close together so that refraction differences are minimized, and which also provide maximum sensitivity. Mook, et al (21) have shown that in the range 200 to 1,000 nm, 810 and 660 nm are optimal with three times the sensitivity of the more frequently used pairs in the 500 to 580 nm range.

History

According to Drabkin and Austin (6), Hufner (their ref.1) first applied spectrophotometry to the study of dilute hemoglobin solutions in 1877. Dilution was necessary because of the high optical density of the pigment. This precluded the possibility of making measurements with hemoglobin in equilibrium with arterial oxygen.

Drabkin and Austin themselves were the first to measure from undiluted blood, but the spectra they obtained, while "fairly

UMI

reproducible for the blood of an individual animal" (p. 111), were sufficiently different from those for hemolyzed blood or crystalline hemoglobin that they did not believe the technique would be useful for measuring oxyhemoglobin saturations in whole, unhemolyzed blood.

In 1942, Millikan (20) first described the ear oximeter, a device that measured the intensity of two appropriate colors of light transmitted through the triangular fossa of the external ear. The intensities of the transmitted colors were correlated with arterial oxyhemglobin saturations determined by van Slyke analysis. Once calibrated, this instrument permitted the first continuous measurements of arterial oxygen saturations in man.

The first report of a spectrophotometric measurement of oxyhemoglobin saturation in an undiluted blood sample collected under anaerobic conditions came from Drabkin and Schmidt (7) who devised a way to hemolyze their samples without exposing them to air. Hemolysis was necessary to reduce the light-scattering caused by red cell membranes. The need for hemolysis caused many difficulties because, regardless of the agent used, hemolysis is seldom complete and the membrane fragments tend to remain suspended to varying degrees and cause inaccurate and inconsistent readings.

In 1949, Brinkman and Zylstra (3) described a technique for making spectrophotometric measurements from undiluted, unhemolyzed blood samples. Instead of measuring the intensity of the light transmitted through the specimen, they measured the intensity of light reflected from it. They made no mention of potential error caused by the light scattering of red cell membranes, but showed that at 100% saturation, there is no change in the reflection values measured from samples with hematocrits ranging from 31 to 72%. This implies that membrane scattering does not affect reflection measurements made from samples within this range.

The work of Keilin and Hartree (17) suggested that reflection spectrophotometry is possible from frozen blood. Quoting Hartridge (their ref. 9), they say that the absorption spectra of twice recrystallized hemoglobin is intensified by cooling in liquid air, and shifted about 5 nm toward the blue.

Anderson, et al (2) developed a technique for measuring oxyhemoglobin saturations using light reflected from whole, frozen blood but their method was never published. Subsequently, Sinha, et al (31) developed a method utilizing light transmitted through frozen blood.

The only published method for measuring oxyhemoglobin saturations with light reflected from frozen blood is that of Gamble, et al (11). They used four discrete wavelengths common to the reflection spectra of hemoglobin and oxyhemoglobin, and applied the intensities of reflection at these wavelengths to a complex equation that can be solved to yield the fractional oxyhemoglobin concentration in the frozen sample.

Microspectrophotometry

Recent interest in microvascular physiology has prompted the development of spectrophotometers attached to microscopes, a development which permits measurement of oxyhemoglobin saturations in small vessels. These devices employ reflected or transmitted light, in either frozen or living tissues. The methods of Anderson (2), Sinha(31), and Gamble (11) mentioned above all employ microscopes. Recently Pittman and Duling (24) developed a transmission method for measuring oxygen saturations in the cheek pouch microvessels of anesthetized hamsters.

Only two of these authors consider the problem of light scattering, either from ice crystals in frozen blood (Sinha) or from red cells in the liquid (Pittman). These considerations are necessary for the equations they use to calculate oxyhemoglobin saturations from the light intensities of the three wavelengths they employ. Further comments on these techniques are in the Discussion of the Microspectrophotometry chapter.

UMI

BULK OXYGENATION OF BLOOD

In order to estimate the extent of precapillary oxygenation in the lung, we must consider the process by which oxygen travels through, and reacts with, a cylinder of blood the diameter of a pulmonary artery or arteriole. This is not the same problem as that in the alveolar capillaries. There, red cells flow through in single file and oxygen diffuses across several tissue barriers including the red cell membrane itself before reaching the hemoglobin within the red cell. The kinetics of this process have been worked out in great detail, but the kinetics of oxygenation of bulk quantities of blood has received less attention.

Theoretically, this problem is analogous to one of simple diffusion. In the case of a cylinder of mixed venous blood surrounded by a gas phase rich in oxygen, we would initially observe the blood to be uniformly dark red. But after some discrete time we would see a rim of bright red oxygenated blood that appeared to widen inward toward the center of the cylinder. Roughton (27) termed the interface between the two states of oxygenated blood an "advancing front." The processes involved in this advance include initial oxygenation of a thin layer of blood adjacent to the vessel wall, followed by diffusion of additional oxygen through this layer to the interface where further conversion of hemoglobin to oxyhemoglobin occurs. As the oxygenated layer widens,

UMI

the distance that oxygen must diffuse to reach deoxygenated blood at the interface increases.

Though this process is one of diffusion plus chemical reaction, Crank (5) has said that it behaves no differently than would a cylindrical system depending on diffusion alone. The diffusion coefficient is merely altered so that the calculated time course of the process matches that which is observed. Crank's remarks were not directed specifically to blood in a vessel, but to the general case of any cylindrical system that depends on the combination of diffusion plus chemical reaction.

Roughton (27) had blood specifically in mind when he derived the Advancing Front Equation to describe the process by which a layer of hemoglobin solution 50-100 um thick becomes saturated with carbon monoxide. This situation is not exactly analagous to that of a cylinder of whole blood exposed to oxygen, yet substitution of the diffusion and solubility coefficients for oxygen into this equation provides the best technique I know of for calculating the extent to which mixed venous blood can be oxygenated in an arteriole.

Marx, et al (19) used the Advancing Front Equation to describe the behavior of blood in a membrane oxygenator and found good agreement between predicted rates of oxygenation and those observed in the conditions for the experimental models they constructed.

UMI

Chapter 3 MICROSPECTROPHOTOMETRY

I built the microspectrophotometer to measure the fractional oxyhemoglobin concentration in the blood vessels of frozen tissue specimens. In this chapter I will describe the components of the instrument, and the tests I conducted to ensure its proper operation.

MICROSPECTROPHOTOMETER - DESCRIPTION

The microspectrophotometer measures the intensity of two discrete wavelengths of light reflected from the surface of frozen blood. Its basic components are: 1) an Illumination System; 2) a Cold Chamber for keeping the blood frozen; 3) an Optical System to confine the measurements to an area 100 µm in diameter; and 4) a Light Intensity Measuring System. The instrument is diagrammed in Figure 3-1.

1. The Illumination System consists of two fiber optic light pipes with illuminators (Keystone Optical Fibers Corp.). The pipes are 91 cm long by 6 mm in diameter. The illuminators employ Sylvania DNF tungsten-halogen lamps that have quartz envelopes, and are powered with a Sola constant voltage transformer to keep the light output constant.

UMI

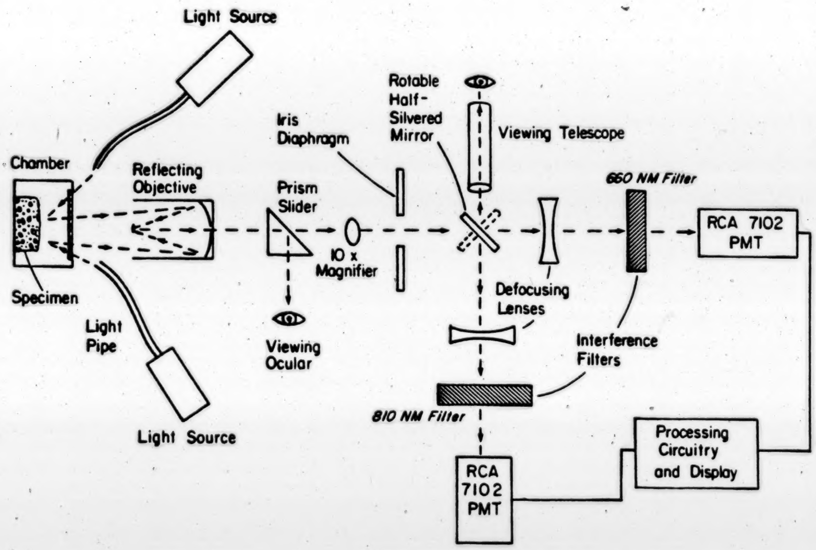
MICROSPECTROPHOTOMETER SCHEMA

Component parts of the microspectrophotometer, and the path the light follows (dashed line) after reflection from the specimen to the light sensitive photomultiplier tubes (PMT).

FIGURE 3-1

The spectral output of the lamps is about 40% greater at 810 nm that at 660 but the effect of this difference is cancelled by adjustment of the amplifiers in the Light Intensity Measuring System.

The light pipes are kept aligned with the specimen by a metal holder fastened to the objective lens of the Optical System.

2. The Cold Chamber is diagrammed in Figure 3-2. It consists of a dry ice reservoir that was machined from solid magnesium. The inner walls are 9.5 cm long by 3.2 cm high by 9 mm thick and are insulated on their outer sides with 1.3 mm thick styrofoam. The chamber plate was machined from a 1.3 cm thick piece of aluminum leaving a 5.1 cm diameter threaded pedestal 6 mm high. The plate is 8 mm thick and of such dimension that it fits into the dry ice reservoir.

A chamber 2.5 cm deep was machined from magnesium tubing, and threaded to screw onto the base plate's pedestal. The top of the chamber is covered with a window of optically flat glass 5.1 cm in diameter by 1 mm thick (Edmund Scientific Products).

Before use, the entire cold chamber is placed in a -30 degree C. cryostat (Harris Refrigeration Inc.). The tissue specimen is placed on the pedestal and the chamber is screwed into place. The chamber plate is placed in the reservoir and the entire assembly is removed from the cryostat and immediately packed with crushed dry ice. A plastic lid covered on its bottom side with 1.3 cm thick styrofoam is

COLD CHAMBER SCHEMA

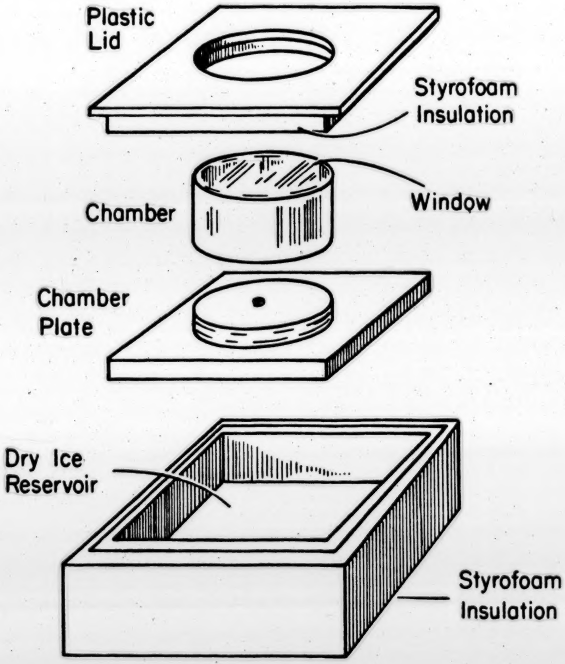

The specimen is placed inside this chamber to keep it frozen while it is on the stage of the microspectrophotometer.

FIGURE 3-2

placed over the reservoir. A hole in the center of the lid accommodates the chamber. The prepared cold chamber is then placed under the illuminators on the stage of the microspectrophotometer where dry air is continuously blown across the optically flat window to keep it free of frost.

3. The light enters the Optical System through a 15X reflecting objective (Beck Inc.) constructed exclusively of mirrors. This device offers the advantages of avoiding the chromatic aberration of lenses, and provides a long working distance (25 mm) from the bottom of the objective to the specimen housed under glass in the cold chamber.

From the objective, the light is deflected by a moveable prism which provides for viewing through binocular eyepieces (10X, Tyoda, Tokyo). The total area viewed is a circle 1.08 mm in diameter.

When the prism is retracted the light passes straight up the microscope tube, through a 10X magnifying lens, through an iris diaphragm in the image plane, and onto a 50% silvered mirror beam-splitter (Ealing Corp.). Half the light thus goes to each of two photomultiplier tubes (RCA 7102). An interference filter in front of each tube permits entry of the light of only the discrete wavelength of interest (810 or 660 nm). The filters are three cavity types with half-intensity bandwidths of about 12 nm, and peak transmissions of about 55%(Ditric Optics Inc.).

UMI

The photomultiplier tubes provide optimum performance when most of their 31 mm diameter photocathodes are illuminated. Because manipulation of the iris diaphragm changes the size of the light spot impinging on the photocathode, an adjustable biconcave lens is placed between each interference filter and the beam splitter to permit modulation of the spot size to the optimum diameter.

Also attached to the beam splitter is a 10X telescope. The beam splitter can be rotated so that half the light is sent through the telescope rather than to one of the photomultiplier tubes. Because it is placed after the 10X magnifying lens and the iris diaphragm, the telescope allows me to determine the diameter of the area of the specimen being viewed by the photomultiplier tubes, and allows adjustment of the iris diaphragm until the desired diameter is obtained. This is usually 100 µm as determined with a micrometer slide placed under the Beck objective. A 50 µm spot is possible but the amount of light reaching the photomultiplier tubes at that setting is too small to provide a reliable signal.

4. The sensors in the Light Intensity Measuring System are two RCA 7102 photomultiplier tubes. They are end-sensing tubes with silver-oxygen-cesium photocathodes 31 mm in diameter. These cathodes will convert 1 watt of light energy into 2.8 mA of electric current; that is they capture 0.43% of the energy in 1 light quantum. Within each tube

is a ten stage amplification system that multiplies the electrical energy produced by the photocathode two hundred thousand times when the tubes are operated at 1250 volts. This voltage is provided by a regulated power supply (Northeast Scientific Corp.).

The electrical signal from each tube is fed into a solid state amplification system that can be continuously adjusted up to 10X. Because the photocathodes are about 25% less sensitive at 660 nm that at 810, this feature allows the signals to be equalized thus balancing out the differences in sensitivity and illuminator output. The amplified signal from each tube is read to the nearest millivolt (1%) on a digital voltmeter. It is these values that are divided one by the other to obtain the 810/660 ratio. A variable bucking current is included in the amplification system to adjust the output signal of each tube to zero when the tubes are not being exposed to the specimen's reflected light (prism in the "viewing" position).

MICROSPECTROPHOTOMETER - TESTS

After construction of the instrument was completed, I tested it in several ways to ensure that it would function properly when analyzing frozen biopsy specimens. These tests were conducted to determine: 1) that the Light Intensity Measuring System responded linearly to changes in light intensity; 2) that the specimen would remain frozen while being illuminated within the cold chamber; 3) that reflection spectra recorded from hemoglobin and oxyhemoglobin were similar to those obtained by other spectrophotometric techniques; 4) that outputs measured with the instrument would produce a linear relationship when plotted against fractional oxyhemoglobin concentration; 5) the minimum thickness of the specimen required to produce reliable data; 6) the effect of differences in hematocrit on the reflection ratios; and 7) whether the ratio measurements drifted with time.

1. Response Characteristics of the Light Intensity Measuring System

The microspectrophotometer was designed to record data that would produce a linear relationship between the 810/660 reflection ratio and percent oxyhemoglobin saturation. If the Light Intensity Measuring System did not respond linearly to changes in light intensity, them correction would have to be applied to the 810 and 660 nm reflection values in order to obtain this relationship. This would introduce error and widen the confidence limits of the measurement. It was important that both photomultiplier tubes respond equally to the same light intensity, or that their amplifiers be adjusted so they appeared to respond equally. Examination of the performance values supplied with each tube by the manufacurer revealed that no two tubes have identical sensitivity. This, combined with the fact that the

UMI

sensitivity of each tube's photocathode is about 25% lower at 660 nm that at 810, and the fact that the illumination system provides light that is slightly less intense at 660 nm than at 810 ensured that the tubes would not provide identical signals for any specific setting of the illumination system.

The adjustable amplifiers were included in the light detecting system so that the effects of these differences could be neutralized. In practice, a magnesium carbonate block is placed on the stage of the instrument for use as a reflection standard. This substance reflects equally at 810 and 660 nm. When the tubes are exposed to light reflected from it, their electrical signals can be equalized by simple adjustment of the amplifiers. Thus all the differences produced by inequalities of sensitivity or illumination can be compensated for.

The linearity of the response was tested by placing a circular optical wedge on the microscope stage and shining light through it into the objective lens. The optical density of the wedge increased continuously around its circumference, so its optical density was proportional to its degree of rotation past a reference point on the stage.

Figure 3-3 is a graph of the percent optical transmission of the wedge plotted against the percent of the maximum response of the Light Intensity Measuring System. The amplifiers were set so that both photomultiplier tubes produced identical responses at the maximum

PHOTOMULTIPLIER TUBE RESPONSE TO

CHANGES IN LIGHT INTENSITY

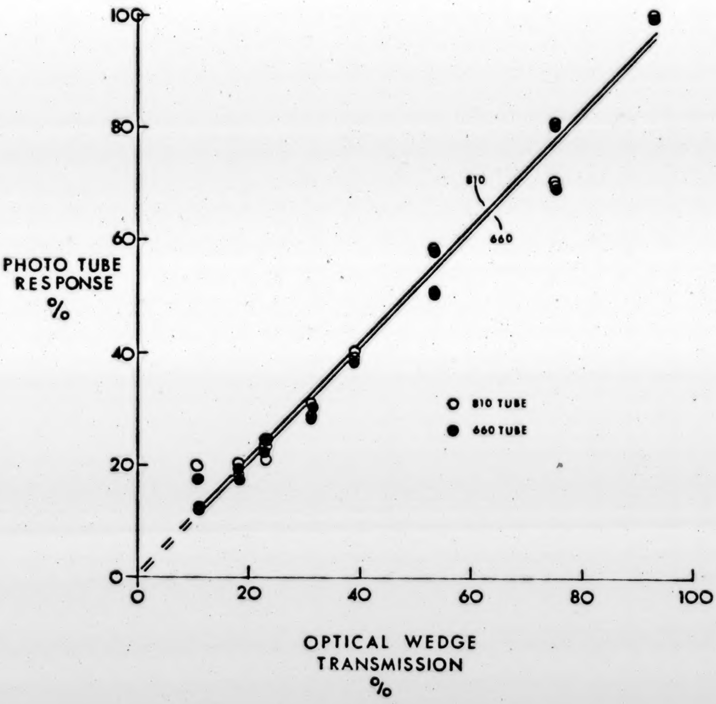

FIGURE 3-3

UMI

transmission of the optical wedge. Hence, 93% transmission of the wedge corresponds to 100% of system response. The lines on the graph are the calculated least-squares regression plots for the data; they were not constrained to pass through the origin. Note that both tubes respond identically when used with the adjustable amplifiers of the system. This means that the ratios of their outputs do not produce compound errors that are greater than the individual errors of numerator and denominator. The slight deviations from linearity at 11% and 93% transmission are probably artifacts resulting from my inability to rotate the optical wedge to precise transmission values; that is, X axis variations may be greater than they appear to be. The identical response of both tubes to the same light intensity means that a linear correlation will be obtained between 810/660 reflection ratio, and fractional oxyhemoglobin saturation if the relationship truly is a linear one.

2. Cold Chamber Stability

The temperature stability of the cold chamber was tested by placing a chromel-alumel thermocouple in the center of the chamber. The reservoir was packed with dry ice and the chamber was placed on the stage of the microspectrophotometer. The illumination system was turned on and the optical system was focused on the previously calibrated thermocouple located within the chamber under the glass

UMI

window. The output of the thermocouple was monitored continuously with the polygraph. I found that the temperature within the chamber remained at -27 degrees C. for about 30 min. After this period, the dry ice had sublimed enough so that an insufficient amount remained to keep the cold chamber chilled. Refilling the reservoir with dry ice caused the temperature to return to -27 degrees C. for another 30 min. period.

Based on these results, I fill the dry ice reservoir about every 20 min. when recording reflection ratios from frozen specimens.

3. Reflection Spectra of Hemoglobin and Oxyhemoglobin

Determination of fractional oxyhemoglobin saturation with the microspectrophotometer is based on known differences in the reflection spectra of hemoglobin and oxyhemoglobin (6). I therefore wanted to make certain that the instrument could measure these spectra accurately from samples of whole, frozen blood.

Pigment samples were prepared by putting 10 ml of heparinized blood into 65 ml stoppered, glass serum bottles. The bottles were placed in a shaker water bath maintained at 37 degrees C., and flushed with 5.6% carbon dioxide in nitrogen, or 5.6% carbon dioxide and 30% oxygen in nitrogen. The bottles were flushed with their respective gas mixtures a total of five times, and shaken for 20 to 30 min. between flushes. At the end of this period 2 samples of blood were drawn from

UMI

each bottle: one into a 1 ml plastic syringe that was immediately frozen in liquid propane (-170 degrees C.); and the other into a 5 ml glass syringe for analysis of pH and oxygen partial pressure. The pH values ranged from 7.2 to 7.3. The oxygen pressures of the deoxygenated samples were always less than 5 torr. This was not a sample of completely deoxygenated hemoglobin, but its true saturation was less than 3%. It was used as zero in these spectral measurements. The oxygenated samples always had oxygen pressures greater than 200 torr and were therefore considered to be 100% saturated.

Specimens of the frozen samples were analyzed with the microspectrophotometer at 6 discrete wavelengths in the range 570 to 810 nm. These data are shown in Figure 3-4. Each data point is the mean of 5 reflection values ± 1 s.d. At 810 nm both samples reflect virtually equally, while at 660 nm the intensities of reflection are maximally different. When compared with absorption spectra in Figure 2-2, the reflection spectra are inverted. Therefore maximum reflection occurs at minimum absorbance. In Figure 2-2 both pigments absorb equally at 810 nm, while at 660 nm their absorptions are maximally different. Light that is not absorbed by an illuminated specimen is either reflected or transmitted. Therefore the reflection spectra I obtained are those I should have obtained if the microspectrophotometer performs accurately.

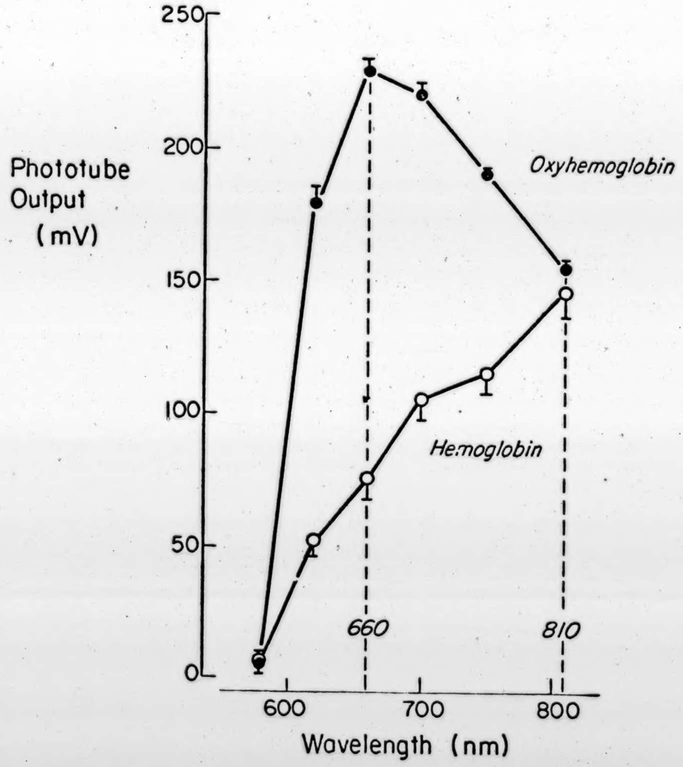

REFLECTION SPECTRA OF FROZEN CAT BLOOD

FIGURE 3-4

4. Linear Relationship Between Reflection Ratio and Fractional Oxyhemoglobin Saturation

A blood sample that was frozen when only partially oxygenated would reflect at 810 nm the same as either hemoglobin or oxyhemoglobin. At 660 nm it would reflect less intensely than oxyhemoglobin but more intensely than hemoglobin. This occurs because such a sample is a mixture of both pigments and its intensity of reflection at 660 nm will be in proportion to the ratio of the pigment concentrations. Enson, et al (9) have shown that the oxygen saturation of liquid blood can be expressed as:

$$\text{Fractional Oxyhemoglobin Conc.} = A \frac{I_{R_{810}}}{I_{R_{660}}} - B$$

where $I_{R_{810}}$ and $I_{R_{660}}$ are the intensities of reflected light at 810 and 660 nm, and A and B are respectively the slope and Y intercept of this linear equation. The derivation of it is shown in the Discussion section of this chapter.

On this theoretical basis I wanted to show that the same linear relationship would obtain for frozen blood when using reflection data measured with the microspectrophotometer. I therefore prepared 5 frozen cat blood samples using the tonometry techniques already described. These samples ranged in oxygen saturation from 0 to 100%, and were prepared with gas mixtures ranging from 0 to 30% oxygen in

UMI

5.6% carbon dioxide and nitrogen. After the period of tonometry was complete, two blood samples were drawn from each tonometry bottle: one was frozen, and the other was analyzed for oxygen content and pH. The pH values ranged from 7.2 to 7.3. The oxygen content of the sample equilibrated with 30% oxygen was assumed to be equal to the oxygen binding capacity of all the samples. The oxygen contents of the other four samples were compared to this and their fractional oxygen concentrations were calculated.

Samples from the frozen samples were analyzed with the microspectrophotometer and the 810/660 reflection ratios of these known samples were plotted against their saturations. This produced curves that could be tested for linearity and confidence intervals.

One such curve is shown in Figure 3-5. Each circle in the plot represents a single reflection ratio measurement, and they are connected by the calculated least-squares regression line. The plot shows that reflection ratios of frozen blood are a linear function of the fractional oxyhemoglobin concentration. The stippled area is the 95% confidence limit of the data and shows that a single reflection ratio is an accurate measure of oxyhemoglobin saturation to ± 10%; multiple ratio measurements significantly improve the accuracy.

Tests were also done using the blood of dogs, sheep, and humans. All yielded data that produced linear graphs when plotted

UMI

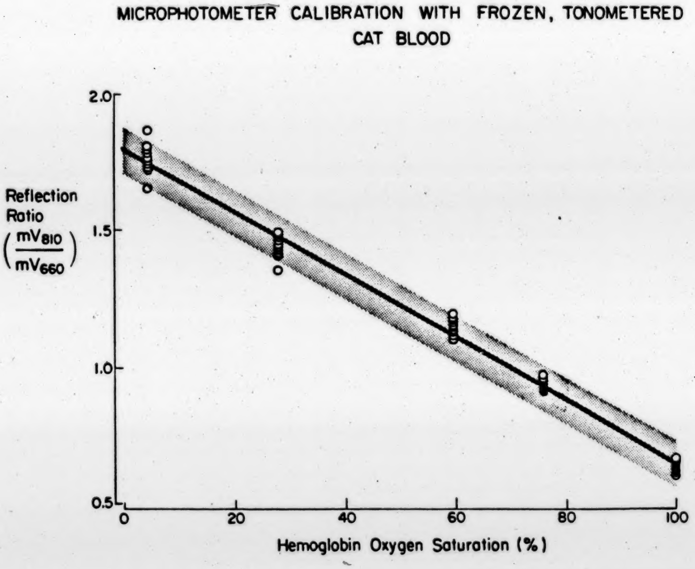
MICROPHOTOMETER CALIBRATION WITH FROZEN, TONOMETERED CAT BLOOD
Reflection Ratio
$\left(\frac{mV_{810}}{mV_{660}}\right)$
2.0
1.5
1.0
0.5
0
20
40
60
80
100
Hemoglobin Oxygen Saturation (%)

FIGURE 3-5

against oxyhemoglobin saturation, and all had 95% data confidence limits equivalent to those in Figure 3-5.

5. Minimum Thickness of Frozen Blood Specimen

In preparing frozen lung specimens for the microspectrophotometer, pulmonary vessels usually are not sectioned perpendicular to their axis of flow. This results in vessel cross sections that are oval. Examination with the microspectrophotometer requires taking measurements from portions of the field adjacent to the wall of these obliquely cut vessels. At such locations the thickness of blood between the surface of the oblique cross section and the wall of the vessel may be very small (Figure 3-6). It was therefore necessary for me to determine the minimum thickness of blood required to produce reliable reflection measurements.

This determination was approached in three ways:

1. A wedge of frozen blood ranging in thickness from 0 to 5 mm was prepared on a microscope slide as follows: A piece of glass 5 mm thick was fixed to the end of the slide and a pool of high or low saturation blood was placed on the slide adjacent to it. A 50 mm cover slip was placed over the pool with one end resting on the slide and the other on the 5 mm

UMI

glass. The wedge was quickly frozen in liquid propane and placed under the microspectrophotometer for measurement.

2. White soda straws were filled with blood of either high or low oxyhemoglobin concentration and quickly frozen in liquid propane. These were sectioned obliquely with the microtome in the cryostat, and the angle between the wall of the straw and the plane of the section was measured. The straw was placed under the microspectrophotometer and reflectance measurements were made sequentially along the long axis of the cross sectional oval. Knowledge of the distance from the sharp edge at which the measurement was made allowed me to calculate the depth of the specimen at that point using the tangent of the angle (Figure 3-6).

3. The third technique was similar to the second except that excised femoral arteries of dogs were used instead of plastic soda straws.

The results of these studies are shown in Figure 3-7. In all three studies the 810/660 ratio is expressed as a percent of the control value, which was the reflection ratio at the specimens' thickest part.

UMI

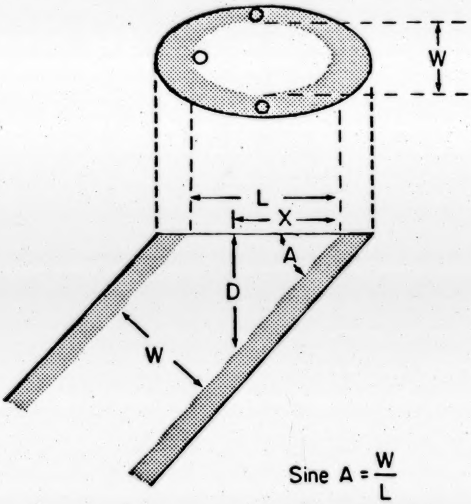

$$\text{Sine } A = \frac{W}{L}$$

$$D = X(\text{TAN } A)$$

A DIAGRAMMATIC VIEW OF THE RELATIONSHIP BETWEEN WIDTH AND DEPTH IN AN OBLIQUELY SECTIONED PULMONARY ARTERY CONTAINING A CORE OF MIXED VENOUS BLOOD AND A RIM OF OXYGENATED BLOOD. THE DISTANCE BENEATH THE SURFACE OF THE CORE (D) CAN BE CALCULATED FROM MEASUREMENTS MADE ON THE SURFACE OF THE CROSS-SECTION. SIMILAR CALCULATIONS FOR THE RIM REVEAL THE DISTANCE FROM THE RIM SURFACE TO THE UNDERLYING VESSEL WALL. THE CIRCLES SHOW THE OPTIMUM LOCATIONS FOR MAKING REFLECTION MEASUREMENTS FROM RIM OR CORE.

FIGURE 3-6

UMI

FIGURE 3-7

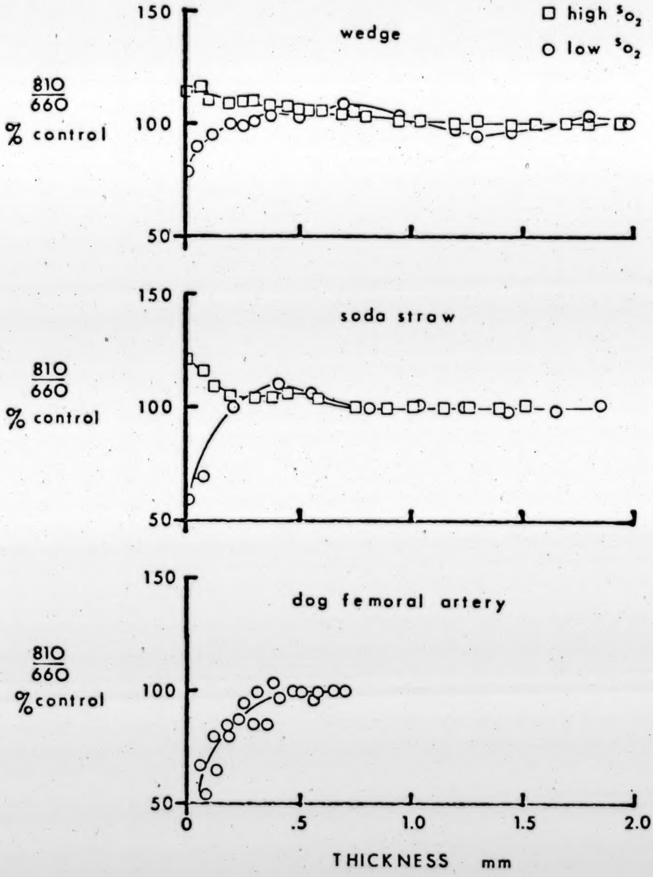

Data showing the minimum thickness of a blood specimen required to obtain reliable reflection ratios, in three different circumstances.

UMI

With the wedge technique, the reflection ratios reach a consistent value (100% of control) at a wedge thickness of about 0.5 mm though deviation from the control value continues in the low saturation sample throughout the range of depths measured. For plastic soda straws the thickness is about 0.7 mm before consistent ratios are achieved, but in the excised dog femoral arteries a constant ratio is obtained at 0.4 mm. Because the dog femoral artery is most like the pulmonary vessels studied in the cat lung experiments, I concluded that the minimum critical specimen thickness is 0.4 mm.

The data in Figure 3-4 predict that a reflection measurement made at 660 nm from an oxygenated blood sample will be the one most sensitive to inadequate specimen thickness. Oxyhemoglobin does not absorb strongly, so this measurement yields the most reflection of any saturation value at either wavelength. Light of this wavelength entering the surface will therefore pass further into the specimen before being absorbed by respiratory pigment and will thus be most likely to be reflected back by an intervening vessel wall. Examination of the 660 and 810 reflection values from these experiments imply that this is so, but the data are inadequate for firm conclusions.

The observation that the minimum thickness of the specimen must be 0.4 mm is therefore an empirical one, but is likely to be correct because it is the value obtained from conditions most like those in experimental use.

UMI

These results also show that the reflection process is not a surface phenomenon, but a result of light interacting with frozen blood beneath the surface. This is important because it means that processes that affect surface smoothness, such as sectioning with the microtome, are not likely to have a strong influence on reflection measurement.

Because reflection occurs from a layer, and not the surface, care must be taken in recording reflection values from obliquely sectioned vessels of small diameter. This situation is illustrated in Figure 3-6, a diagram of a vessel that contains a rim of oxygenated blood surrounding a core of deoxygenated blood. The figure shows that reflection measurements made from the core could be affected by the underlying rim. Dimensions that can be measured in the plane of the section allow calculation of the angle at which the vessel was cut, and hence calculation of the point on the surface of the core where the depth is adequate. The depth of the rim can be determined similarly, but curvature of the vessel wall is a complicating factor. Calculations for a vessel 0.5 mm in diameter, the smallest I used for making reflection measurements, show that with a rim 100 µm wide, the vessel can be cut at an angle up to 68 degrees (angle A in Figure 3-6) and there will still be sufficient depth and surface area for making reflection measurements from spots 100 µm in diameter in both rim and core. For larger vessels the minimum acceptable angle of section is smaller; if a vessel with a rim 150 µm wide was cut longitudinally down

UMI

the middle (angle A=0), its minimum diameter would have to be about 2 mm to yield reliable reflection data from the rim because of curvature of the vessel wall. The core radius would be 850 µm, more than twice that necessary to produce reliable reflection data.

6. Effect of Hematocrit

Blood samples of different hematocrits have different concentrations of light absorbing and reflecting pigments, and might therefore be expected to yield different results with the microspectrophotometer even in samples of the same fractional oxyhemoglobin concentration.

I tested this possibility by reconstituting samples of sheep blood to various hematocrits ranging from 0 to 50, and then equilibrating them with 5% carbon dioxide in either oxygen or nitrogen. The samples were frozen in liquid nitrogen and analyzed with the microspectrophotometer. The results are shown in Figure 3-8.

In the figure, the high and low oxyhemoglobin saturation data are plotted separately. Each data point is the mean of 5 reflection ratios ± one s.d. The lines were fitted by eye with the aid of a French curve. The reflection ratio recorded at the highest hematocrit for each condition of oxygenation is used as the control value for that condition. This makes it appear as if the reflection ratio of plasma (hematocrit =0) is dependent on its state of oxygenation, but this is

EFFECT OF CHANGES IN HEMTOCRIT ON
810/660 REFLECTION RATIO

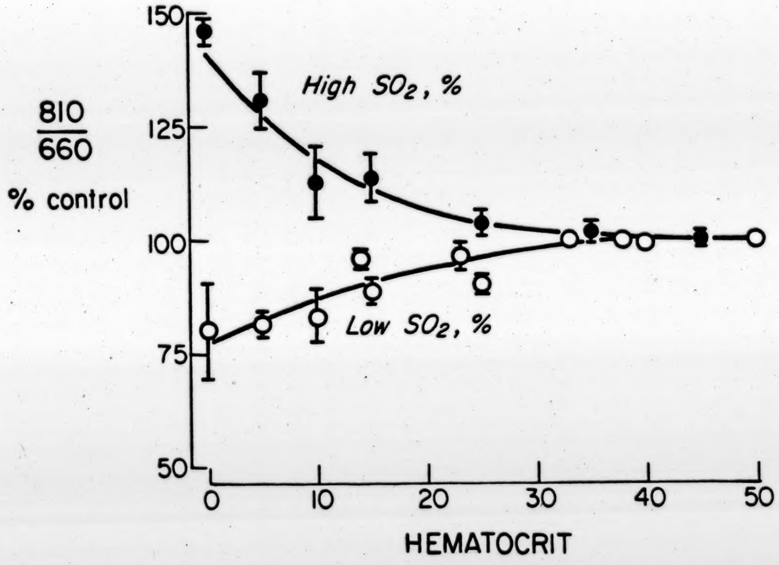

FIGURE 3-8

an artifact of the way the data is expressed; before being normalized the reflection ratios for plasma were identical regardless of their state of oxygenation.

The data show that the reflection ratio does not change with the hematocrit in the range 30 to 50. This means that the reflection ratios of samples of different hematocrits can be compared if they are within this range. In my animal experiments the hematocrits were always greater than 34; also, microspectrophotometer measurements were compared only within experiments, not between them. Therefore, errors due to differences in hematocrits would never have arisen anyway. Even if there were local differences in hematocrit within an individual lung lobe, the data suggest that the values would have to have fallen below 30 for the reflection ratios to have been affected.

7. Stability of Reflection Ratio Measurements

I wanted to determine whether the reflection ratios drifted with time under two conditions: 1) while the specimens were in the cold chamber on the stage under the illumination system; and 2) after the specimens had been stored in liquid nitrogen for several weeks.

a.) I checked the first condition by placing a specimen of frozen blood in the cold chamber on the stage of the microspectrophotometer and connecting the output of the amplification system to the polygraph.

UMI

The cold chamber was kept filled with dry ice, and the bucking current was adjusted periodically to ensure that the base line of the phototube response did not change. Under these conditions there was no detectable change in either the 810 or the 660 nm signal over a period of nearly 3 hrs. The only drift that did occur was in the base line. Detectable base line deviations occur in the 810 nm tube after 20 min., and in the 660 nm tube after about 50 min. This deviation is neutralized by simple adjustment of the bucking current in the amplification system, and is checked frequently during normal operation of the instrument.

b.) Long term aging of the specimens was tested by recording reflection data from tonometry samples that had been stored in liquid nitrogen (as are all tissue specimens studied with the microspectrophotometer). Comparison of the linear regression plots for these samples on the day after they had been prepared with those 6 weeks later showed no siginificant differences in confidence limits of the data or the regression lines. There were minor differences in intercept values due to variations in calibration but there were no significant differences in slope.

MICROSPECTROPHOTOMETER - OPERATING PRACTICES

I make oxyhemoglobin saturation measurements with the microspectrophotometer using the following procedures:

The specimens are removed from liquid nitrogen storage and placed in the cryostat at -30 degrees C. for about an hour to warm. During this period the power supply for the photomultiplier tubes is turned on and allowed to stabilize at a constant output of 1250 V, and the illumination system is turned on so the lamps can stabilize at a constant spectral output. The diameter of the image plane diaphragm is set to 100 µm using a micrometer slide and the telescope attached to the beam splitter. After the warm-up period is complete, a magnesium carbonate block is placed in focus on the stage and light reflected from it is used to generate signals in both photomultiplier tubes. The amplifiers in the Light Intensity Measuring System are adjusted so that both tubes indicate maximum equal output.

At the end of each animal experiment a mixed venous and an arterial blood sample are drawn for oxygen saturation determination in our Physiological Services Laboratory, and a fraction of each sample is rapidly frozen. In these experiments one lobe of the animal's lung is ventilated with 100% oxygen and the remainder of the lung is ventilated with 30% oxygen. This produces mixed venous oxyhemoglobin saturations of 30%, arterial saturations of 70%, and assumed saturations of 100% in the veins of the oxygen ventilated lobe (Chapter 4). Portions of these

3 frozen samples are used for daily calibration of the microspectrophotometer.

Once these tissues have equilibrated in the cryostat, fractions of each are finished to a smooth surface with the microtome and examined with the microspectrophotometer. Ten reflection ratio readings are taken from each. Using a Hewlett-Packard 9100B desk-top computer, a least squares linear regression plot is made of the reflection ratios versus their respective saturation values. A typical example is shown in Figure 3-9. In the figure, the outer pair of lines is the 95% confidence limits of the data, and inner pair is the 95% confidence limits of the regression.

Once this calibration plot is completed, the instrument is ready to record data from frozen vessels of unknown oxyhemoglobin saturations. For each saturation determination, 5 reflection ratios are recorded and the mean and 95% confidence limits are calculated. These values are applied to the Y axis of the calibration plot, and with the use of the regression line and its confidence limits the mean oxyhemoglobin saturation and its 95% confidence limits are read on the X axis (Figure 3-9). The example in the figure is representative of recorded experimental data, and shows that a saturation value determined this way has 95% confidence limits of ± 5%.

UMI

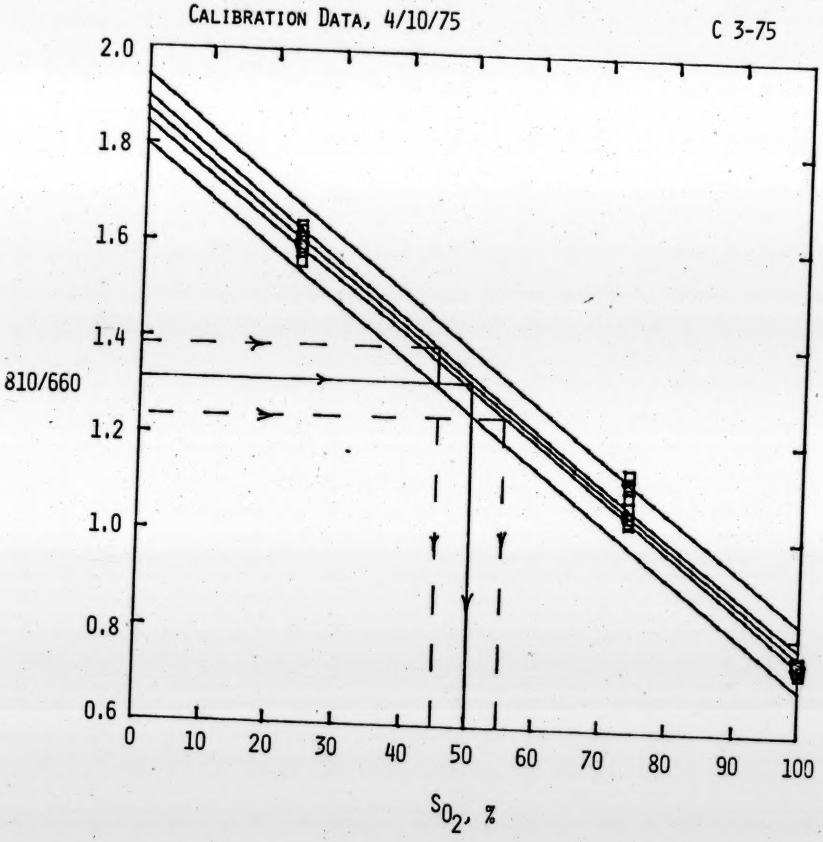
CALIBRATION DATA, 4/10/75
C 3-75
2.0
1.8
1.6
1.4
1.2
1.0
0.8
0.6
810/660
0
10
20
30
40
50
60
70
80
90
100
S_{O_2}, %

FIGURE 3-9

MICROSPECTROPHOTOMETER - DISCUSSION

The basis for the linear equation relating 810/660 reflection ratio to fractional oxyhemoglobin saturation is as follows (from Enson, et al (9)):

If I_o is the intensity of incident light shown on a reflecting or refracting medium such as blood, and if I_R is the intensity of the light refracted, or reflected back, then the following relationship has been shown to exist (1):

$$I_R = I_o \frac{d_x}{2e_x} \qquad 1.$$

where x is the wavelength of I_o , and d and e are respectively the specific scattering and extinction coefficients at that wavelength. e is assumed to be much larger than d.

Because blood consists of two pigments,

$$e_x = (C_{Hb_x} e_{Hb_x} + C_{O_2Hb}\, e_{O_2Hb_x}) \qquad 2.$$

where C_{Hb} and C_{O_2Hb} are the fractional concentrations of hemoglobin and oxyhemoglobin respectively.

Substituting equation 2 into equation 1, and considering the use of two wavelengths, we get two equations as follows:

UMI

$$I_{R_{660}} = I_{o_{660}} \frac{d_{660}}{2(C_{Hb}\, e_{Hb_{660}} + C_{O_2Hb}\, e_{O_2Hb_{660}})} \qquad 3.$$

$$I_{R_{810}} = I_{o_{810}} \frac{d_{810}}{2(C_{Hb}\, e_{Hb_{810}} + C_{O_2Hb}\, e_{O_2Hb_{810}})} \qquad 4.$$

Dividing equation 4 by equation 3, and assuming that $e_{Hb_{810}} = e_{O_2Hb_{810}}$ (isosbestic point; see Figure 3-4), that $C_{Hb} + C_{O_2Hb} = 1$, and that $I_{o_{660}} = I_{o_{810}}$ (calibration utilizing MgCO block):

$$C_{O_2Hb} = \frac{I_{R_{810}}}{I_{R_{660}}} \frac{d_{660}\; e_{810}}{d_{810}\;(e_{O_2Hb_{660}} - e_{Hb_{660}})} - \frac{e_{Hb_{660}}}{(e_{O_2Hb_{660}} - e_{Hb_{660}})} \qquad 5.$$

or

$$\text{Fractional HbO}_2 \text{ Conc.} = A \frac{I_{R_{810}}}{I_{R_{660}}} - B \qquad 6.$$

where A and B are the slope and intercept, and are determined by the extinction and diffusion coefficients for the two pigments at each wavelength.

As shown here, the equation applies only to the isosbestic and differential wavelengths of 810 and 660 nm, though any combination of such wavelengths will do. They are usually chosen to be as close to each other as possible to minimize refraction differences. Figure 1-1 shows that several other combinations are available in the range 520 to

580 nm, though Mook, et al (21) have shown that the differential wavelength at 660 nm offers measurement sensitivity 3 times greater than those in the range 520 to 580 nm.

Equation 6 can be used to calculate fractional oxyhemoglobin concentrations from measurements of $I_{R_{810}}$ and $I_{R_{660}}$ if A and B are known, and several workers use spectrophotometers attached to microscopes in this way (24, 25, 31). This technique requires a one-time empirical determination of A and B through the use of several dozen blood samples of known oxyhemoglobin saturation. Once these values have been found, they are used in all future calculations of saturation.

This technique is further complicated by the fact that a measured value of I_R = true I_R + T, where T is a nonspecific scattering term caused by the presence of red cell membranes, ice crystals, and other particulates that make blood different from the transparent solutions to which the Lambert-Beer Law can be directly applied. Therefore, calculation of fractional oxyhemoglobin concentration with equation 6 requires knowledge of the value of this term. The equation can be re-written to express this as follows:

$$\text{Fractional } O_2\text{Hb Conc.} = A\ \frac{mI_{R\ isos} + T_{isos}}{mI_{R\ diff} + T_{diff}} - B \qquad 7.$$

where $mI_{R\ isos}$ and $mI_{R\ diff}$ are the measured light intensities at the isosbestic and differential wavelength respectively.

Pittman and Duling (24,25) and Sinha, et al (31) have a technique for experimentally determining T from one differential and two isosbestic wavelengths that are all of nearly the same value (520, 546, and 555 nm). This is necessary so that the refraction differences among the 3 are minimized. When this condition is satisfied, they assume that $T_{isos\ 1} = T_{isos\ 2} = T_{diff}$. This value is applied to equation 7 so that the calculation can be completed. These 3 wavelengths appear to be the only ones suitable for use in equation 7.

My technique is superior is several respects:

1. It utilizes a differential wavelength that provides a sensitivity of measurement 3 times greater than that available in the 520-580 wavelength region.

2. It requires measurements of I_R at only 2 wavelengths instead of 3.

3. It utilizes a calibration plot that is conveniently drawn each time the instrument is used; that is made with data from

UMI

the experimental animal's own blood; and from which oxyhemoglobin saturation values are read directly without calculation. It does not depend on one-time measurements of slope and intercept that are subject to drift.

I make no attempt to correct for scattering. Such a correction is not necessary because saturation values are determined empirically from a calibration plot that I have shown to be a linear expression of 810/660 reflection ratio versus percent oxyhemoglobin saturation. A separate term for scattering need not be considered.

Statistical Methods

In making saturation determinations by means of reverse regression from my calibration plots (Figure 3-10), I wanted to utilize a formal statistical method; I therefore sought the advice of a statistician. He attempted to make use of a method developed by Scheffé (30) that provides a way to conduct reverse regression and also find the confidence limits of the results. It was difficult to apply this technique to my specific calibration plots because the data I use to construct them consistently has more variation at low saturation values than at high ones. The cause of this inequality is unknown but it prevents the formal application of Scheffé's method. My technique for finding the mean oxyhemoglobin saturation and the 95% confidence limits of an experimental sample is therefore partly empirical, but when compared to a Scheffé model in which the variance was assumed to be equal, no significant difference was found between means and confidence limits determined by that technique and by my own.

UMI

Chapter 4 CAT EXPERIMENTS

INTRODUCTION

After having shown that the microspectrophotometer could accurately measure oxyhemoglobin saturations in blood prepared by tonometry, I began animal experiments. I first showed that the instrument could accurately measure oxyhemoglobin saturations in the blood within the vessels of isolated, perfused cat lungs. I then prepared frozen cat lungs under conditions that were optimal for precapillary oxygenation and showed that such oxygenation did occur under the conditions of the experiments. I did three experiments in which these conditions were altered and showed their effect on the degree of precapillary oxygenation. I eventually concluded that these experiments did not permit me to determine the extent of this process in normal, unfrozen lungs, so I constructed models to estimate it. The models are described in the next chapter.

ISOLATED, PERFUSED CAT LUNG EXPERIMENTS

The microspectrophotometer was built to measure the fractional oxyhemoglobin concentration in the blood of frozen cat lungs. I had shown that it could accurately measure such concentrations in blood frozen after tonometry, but I needed to show that in vivo microspectrophotometry would produce similar results. I investigated this by preparing frozen cat lungs that had uniform oxyhemoglobin saturations throughout their circulatory systems. Thus the one variable I wanted to measure in subsequent experiments was eliminated and variables due to any other causes would be revealed.

Anesthetized, open thorax cats were exsanguinated and the shed blood was heparinized. Cannulas were placed in the left atrium and pulmonary artery and the lungs were perfused at room temperature with a Cole-Parmer Masterflex roller pump. The pump was set so that the perfusion pressure was equivalent to the animal's pulmonary arterial pressure before it was killed. The lungs were ventilated with either high or low oxygen mixtures containing 5.6% carbon dioxide. When the oxygen partial pressure of PA and LA blood differed by less than 5 torr, I quickly froze the lungs with liquid propane and assumed the oxyhemoglobin saturation was identical in arteries and veins.

The results are shown in Table 4-1. There was no need to convert the 810/660 reflection ratios to oxyhemoglobin saturations since only distribution and variance measurements were considered. In 5 studies the average standard deviation was 7.9% of the mean value found within individual vessels of each lobe. The deviation was not any different at high oxyhemoglobin saturations than at low ones. When this deviation is related to a typical calibration plot, as in Figure

REFLECTION RATIOS FROM FROZEN BLOOD VESSELS IN 5 ISOLATED-PERFUSED CAT LUNG LOBES

810/660 Reflection Ratios

DATE	P_{O_2} PERFUSATE, TORR	WITHIN VESSELS				BETWEEN VESSELS			
		MEAN	C.V.	95%CONF	N	MEAN	C.V.	95%CONF	N
10/1	38	1.432	5.7%	1.2%	87	1.430	5%	2.5%	18
10/8	34	1.588	8.1%	1.5%	127	1.574	7.9%	3.0%	29
10/15	198	0.802	5.7%	1.0%	143	0.805	5.5%	2.0%	32
10/30	43	1.495	10.8%	1.5%	198	1.498	7.4%	2.4%	43
11/13	8	1.854	9.4%	1.4%	170	1.843	9.8%	3.2%	37
	MEAN		7.9%	1.3%			7.1%	2.6%	

Table 4-1

UMI

3-9 (the in vitro measurement) it corresponds to an average oxyhemoglobin saturation deviation of ± 9%. This correlates well with the 95% confidence limits of the data in that plot which are of about the same value.

Because of the large numbers of readings in each study, the 95% confidence limits of the mean are much smaller than the standard deviation. The average was 1.3% of the mean. This corresponds to only 1.5% saturation units in Figure 3-10 which is about the same as the 95% confidence limits of the regression line there.

The most important result of these experiments is that they show that the deviation in the between vessel readings is not markedly different from that within vessels! This means that the variability seen is about the same in all vessels read, and is not due to real oxyhemoglobin saturation differences from vessel to vessel within a specific lobe. The deviations are therefore simply random errors in measurement and should not cause the results of in vivo measurements to be different from those made in vitro.

A one-way analysis of variance in each experiment shows that the mean reflection ratios from each vessel are not from the same statistical population. This does not alter our conclusions because the variation of the means is smaller than the variation of the data in Figure 3-9. The microspectrophotometer does not measure oxyhemoglobin saturations precisely enough to resolve the differences suggested by the variations in the mean reflection ratios.

PRECAPILLARY OXYGENATION EXPERIMENTS (100% OXYGEN)

Animal Preparation

Cats weighing from 3 to 4 kg were anesthetized with intravenous sodium pentobarbital (30 mg/kg). They were placed supine and plastic cannulas were inserted into a femoral artery and vein. Saline was slowly dripped into the vein to prevent dehydration during subsequent preparations or surgery.

A double-barrel, concentric lumen cannula was placed into the trachea (see Figure 4-1). The animal was paralyzed (20 mg gallamine triethiodide (Flaxedil), I.V.) and ventilated through the tracheal cannula with air or oxygen. Inspiratory pressure was maintained with a water seal set to a depth of 10 to 15 cm.

The animal's chest was opened with an incision down the midline of the thorax and with lateral incisions just rostral to the diaphragm extending from the thoracic midline to the spine. The resulting flaps of chest wall were tied back to expose the thoracic contents widely. After the initial thoracic incision, expiratory pressure was adjusted to 5 cm water with an additional seal.

UMI

After careful dissection of the pleura at the bases of both left and right lower lung lobes, ties were loosely placed around the main bronchi of each lobe. The inner barrel of the tracheal cannula was advanced until its tip was in the main bronchus of a lower lobe. It was tied securely in place. The contralateral lobe was left untied and served as a control since the low gradient between its alveolar gas and pulmonary arterial blood would not lead to any detectable precapillary oxygen uptake (Figure 4-1). Inspiratory and expiratory pressures were maintained in the isolated lobe with water seals set to the same values as the remainder of the lung.

The cannulated lobe was ventilated with 100% oxygen and the remainder of the lung was ventilated via the outer barrel of the cannula with 7% oxygen in nitrogen. This depressed the animal's mixed venous oxygen partial pressure so that blood entering all lobes had a low oxygen content. The presence of 100% oxygen in the alveolar gas of the isolated lobe coupled with the low venous oxygen pressure provided optimum conditions for oxygenation of precapillary blood (Figure 4-1).

The pericardium was cut and reflected and a P.E. 90 polyethylene cannula was passed through the wall of the right ventricle and into the main pulmonary artery. It was secured with a purse string suture in the ventricular wall. This portal allowed sampling of mixed venous blood.

UMI

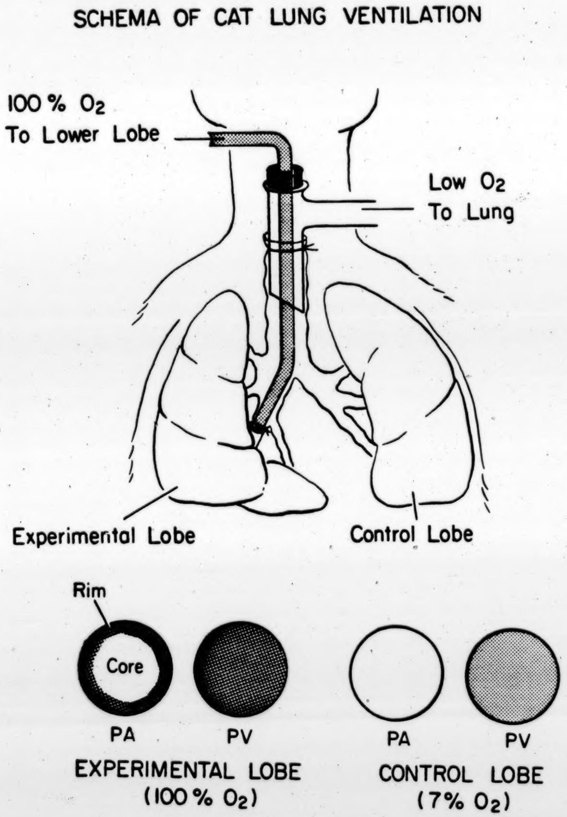

Cat lung ventilation technique and its effect on oxygenation (stipling) in "experimental" and "control" lobes.

FIGURE 4-1

After steady state conditions of gas exchange were established, as determined by periodic arterial sampling, two anaerobic samples of each of pulmonary and femoral arterial blood were drawn. One sample from each vessel was placed in ice water for subsequent analysis in the Physiological Services Laboratory for determination of oxygen content and capacity, and pH. The remaining samples were frozen in liquid propane for later use in calibrating the microspectrophotometer.

The animal's lungs were quickly frozen by flooding the open thorax with liquid propane (-170 C.) according to the technique of Staub and Storey (36). After the lungs were frozen solid, the two lower lobes were excised and placed in liquid nitrogen (-196 C.) where they were stored until ready for measurement with the microspectrophotometer.

Results

Four experiments of this type were completed. The lobe ventilated with 100% oxygen was termed the "experimental lobe" and the contralateral one the "control lobe." Photographs of sections from both types are shown in Figure 4-2.

About half of the pulmonary arteries of the "experimental lobes" contained dark cores indicative of poorly oxygenated blood. These were surrounded with rims of bright red, well oxygenated blood. Microspectrophotometric oxyhemoglobin saturation measurements were made

UMI

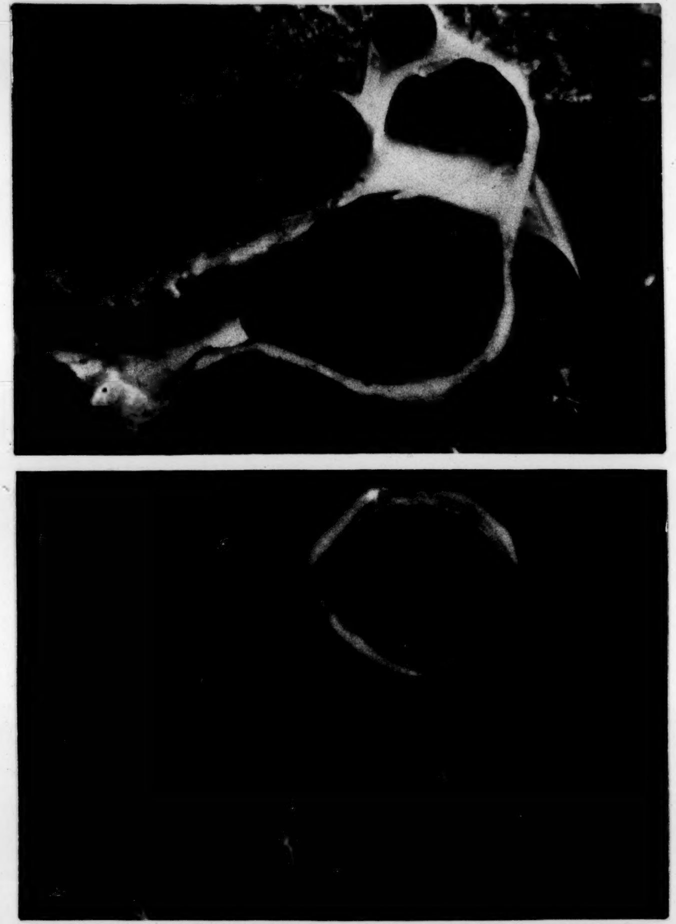

Sections from frozen "control" (top) and "experimental" (bottom) cat lung lobes. Pulmonary arteries (PA) and pulmonary veins (PV)are visible. Note the dark, poorly oxygenated blood that fills the artery of the "control" lobe, and the red, oxygenated blood in the vein.

The red rims in the arteries of the "experimental" lobe indicate that blood entering the lobe has been partially oxygenated, even before arrival at the capillaries.

See text for details of animal preparation. 15X.

FIGURE 4-2

UMI

from both cores and rims. In the pulmonary arteries of the "control lobes" no rims were seen, and therefore only core measurements were made in the first three experiments. In the fourth, measurements were made from the region adjacent to the vessel wall to verify that rims did not form.

Diagrammatic results of a typical experiment (2) are shown in Figure 4-3. Tabular results for all four are in Table 4-2. The data for the "experimental" and "control" lobes are presented separately. In each lobe oxyhemoglobin saturation values for arteries and veins are shown with the arteries of the "experimental lobes" further divided into cores and rims. This subdivision is also given for the arteries of the "control lobe" of Experiment 4.

Reflection spectrophotometric oxyhemoglobin saturation measurements were also taken from the pulmonary veins in both lobes. These values in the "control lobes" were consistent with their having been ventilated with 7% oxygen. This was also true of the oxygen ventilated "experimental lobes."

The most significant result is that the rims of the arteries in the "experimental lobes" had saturation values significantly higher than their cores as determined by Bonferroni paired t test((4); see discussion). It is important to note that "n" values in the rims and cores of the "experimental lobes" are not equal, due to lack of rim formation in some arteries (see "General Discussion" chapter). But, in

UMI

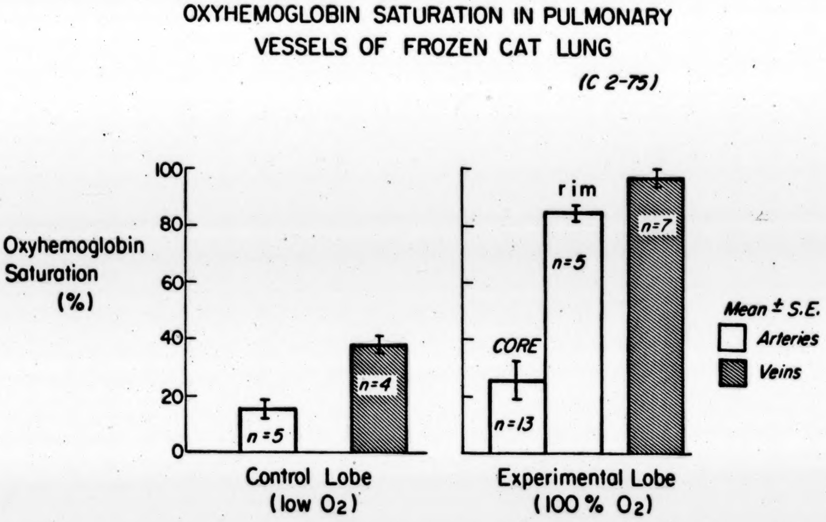

FIGURE 4-3

UMI

OXYHEMOGLOBIN SATURATIONS IN FOUR FROZEN CAT LUNGS

(Experimental Lobes Ventilated with O_2 before Freezing)

MEANS ± S.E. (%)

	Control Lobe			Experimental Lobe		
CAT NO.	ARTERIES		VEINS	ARTERIES		VEINS
				CORES	RIMS	
C 1-75	52.6 ± 2.7 (18)*		70.8 ± 4.3 (12)	56.5 ± 4.5 (23)	87.7 ± 2.3 (12)	94.8 ± 1.3 (9)
C 2-75	15.4 ± 3.1 (5)		36.8 ± 3.5 (4)	26.8 ± 6.1 (13)	84.3 ± 2.6 (5)	98.5 ± 1.0 (7)
C 3-75	28.2 ± 1.6 (8)		45.5 ± 1.0 (2)	46.7 ± 3.7 (14)	66.7 ± 5.3 (6)	99.2 ± 0.64 (10)
	CORES	RIMS				
C 4-75	51.7 ± 3.1 (17)	57.0 ± 1.9 (15)	85.9 ± 2.0 (14)	41.9 ± 2.4 (14)	53.4 ± 2.0 (14)	93.4 ± 4.1 (7)

* No. of observations

TABLE 4-2

the conditions of these experiments, oxygen does enter precapillary blood in a significant number of vessels.

FREEZING TIME EXPERIMENTS

I thought the size and extent of rim formation in the "experimental lobes" might be dependent on the time the blood spent in the pulmonary arteries before being frozen. I decided to study this question by measuring the freezing time of cat lung lobes.

I prepared cats as before except that in one lower lobe I inserted 0.1 mm diam. copper-constantan thermocouple wires. The output of the thermocouples was continuously recorded with the polygraph while the lungs were frozen with liquid propane or liquid nitrogen. After freezing was complete the lobes were removed from the animal and placed in the cryostat where the tips of the wires were dissected out. I measured the distance from the surface onto which the freezing agent was poured to the thermocouple tip.

In Figure 4-4 these values are plotted versus the time it took each thermocouple to reach 0 C. Not only was freezing not instantaneous, as I had previously assumed, but the freezing time was a function of the depth of the thermocouple placement within the lobe. This meant that deeper pulmonary arteries have longer times to absorb oxygen before they are frozen solid.

TIME FOR THERMOCOUPLES TO REACH 0^{o}C. IN A CAT LUNG LOBE BEING FROZEN WITH LIQUID PROPANE OR LIQUID NITROGEN

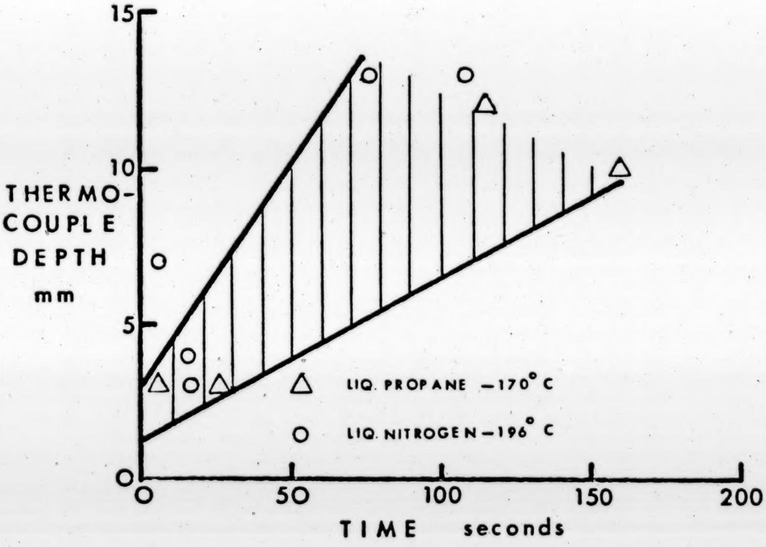

FIGURE 4-4

CLAMPED HILUM EXPERIMENT

I tested the hypothesis that the rim size is proportional to the time the blood spends in the precapillary vessels by preparing a cat similarly to those in Experiments 1 through 4, except that the vessels at the hilum of the "experimental lobe" were clamped just before freezing was started. The blood was therefore stagnant in all vessels of this lobe during the freezing period. The lobe was continuously ventilated with 100% oxygen until freezing was complete.

Both lower lobes were removed and examined in the cryostat. All vessels in the "experimental lobe" were filled with bright red blood. No dark cores were present. Oxyhemoglobin saturation measurements made with the microspectrophotometer from rim and core regions of several pulmonary arteries revealed no detectable difference in saturation. The pulmonary arteries of the "control lobe" (left unclamped during freezing) appeared to have no rims yet the microspectrophotometer revealed a significant difference between rim and core saturations (Table 4-3).

In this experiment the blood remained unfrozen in the precapillary vessels of the "experimental lobe" long enough to be completely oxygenated. This suggested that the size of the rims seen in the first four experiments was partially the result of the time the blood spent in the precapillary vessels before being frozen.

OXYHEMOGLOBIN SATURATIONS IN A CAT LUNG LOBE WITH HILAR VESSELS CLAMPED JUST BEFORE FREEZING WAS STARTED

MEANS ± S.E. (%)

CONTROL LOBE			EXPERIMENTAL LOBE		
ARTERIES		VEINS	ARTERIES		VEINS
CORES	RIMS		CORES	RIMS	
21.5 ± 2.5 (11)*	30.8 ± 1.9 (11)	32.4 ± 3.5 (6)	94.4 ± 1.3 (9)	94.5 ± 1.1 (9)	97.1 ± 1.0 (9)

* NO. OF OBSERVATIONS

TABLE 4-3

UMI

PRECAPILLARY OXYGENATION EXPERIMENTS (AIR)

Because the extent of rim formation in the previous experiments was proportional to the time the mixed venous blood spent in the precapillary lung vessels, it seemed that it should also be proportional to the oxygen partial pressure difference between alveolar gas and mixed venous blood.

I tested this hypothesis by preparing two cats in the usual manner except that the "experimental lobes" were ventilated with air (alveolar oxygen pressure = 100 torr) instead of 100% oxygen. (The remainder of the lung was ventilated with 10% oxygen instead of the usual 7% to keep the animal from dying from hypoxemia.) The results (Table 4-4) show that the rims of the arteries in the "experimental lobes" had oxyhemoglobin saturations significantly higher than those in the cores, yet the rim values were less than those of the veins in that lobe. (Discussion section, this chapter).

I measured the width of the rims in the "experimental lobes" and compared them with similar measurements taken from photographs of the "experimental lobes" in experiments 1 through 4. The mean values ± 1 s.d. are shown in Table 4-5. The rims of the air-ventilated lobes were only 1/6 the width of those in the lobes ventilated with 100% oxygen confirming that the oxygen partial pressure difference between alveolar gas and mixed venous blood influences the size of precapillary pulmonary arterial rims.

UMI

OXYHEMOGLOBIN SATURATIONS IN 2 FROZEN CAT LUNGS.
"EXEPRIMENTAL LOBES" VENTILATED WITH AIR BEFORE FREEZING

MEANS ± S.E. (%)

	CONTROL LOBES		EXPERIMENTAL LOBES		
CAT NO.	ARTERIES	VEINS	ARTERIES		VEINS
			CORES	RIMS	
C 6-75	34.9 ± 1.9 (10)*	87.1 ± 1.1 (7)	47.2 ± 3.2 (10)	70.9 ± 4.5 (10)	99.1 ± 1.7 (3)
C 7-75	66.0 ± 2.0 (9)	95.5 ± 0.8 (5)	66.9 ± 2.9 (12)	76.9 ± 2.8 (12)	97.0 ± 1.7 (3)

* NO. OF OBSERVATIONS

TABLE 4-4

WIDTHS OF OXYGENATED RIMS IN PULMONARY ARTERIES OF
FROZEN CAT LOBES
VENTILATED WITH OXYGEN OR AIR BEFORE FREEZING

MEANS ± S.D. (UM)

Ventilating gas	
100% O_2	AIR
401 ± 138 (32)*	62 ± 30 (22)

* No. of observations

Table 4-5

DISCUSSION

These experiments prove that blood in the pulmonary arteries and arterioles can be oxygenated before reaching the pulmonary capillaries. They also show that the extent of this process is strongly influenced by the time available for it to occur, and by the gradient of oxygen concentration (oxygen partial pressure) from alveolar gas to pulmonary arterial blood. The experiments do not demonstrate how extensive this phenomenon is under normal physiological conditions.

The freezing time experiments show that freezing takes far too long to measure any rim formation that might be present in a normal lung. The estimated time required for blood to flow from the main pulmonary artery to the pulmonary capillaries is less than 1.5 sec (10,29). Because the freezing times in my experiments were as long as 160 sec, the size of the rims I saw is markedly enhanced, and therefore not representative of the expected rim size for normal lungs. I made no attempt to correlate rim size in a specific vessel with the time it took that vessel to freeze. Such a relationship undoubtedly exists but knowing it would provide no useful information. It is sufficient to know simply that rim size is proportional to freezing time.

No attempt was made to determine the exact nature of the relationship between rim size and alveolar oxygen partial pressure. It is sufficient to have shown that such a relationship exists (Table 4-5) without determining it specifically.

These relatively few experiments are sufficient to show that precapillary oxygenation does take place. A greater number of experiments would provide no further information about how much this process occurs in a normal lung. I completed several calculations to estimate the extent of the process normally, and they are described in the next chapter.

Precapillary Oxygenation Experiments (Air)

In these experiments, saturation values for the rims of the arteries in the "experimental lobes" appeared to be less than those of the veins in those lobes (Table 4-4). This was due to the narrow width of the rims in the arteries. The microspectrophotometer measures from an area 100 µm in diameter, but since the average rim in those vessels was 62 µm wide (Table 4-5) saturation measurements from the rim included portions of the poorly oxygenated core. This makes the oxygen saturation of the rims appear to be low in those experiments. In spite of this, there was a significant difference in oxyhemoglobin saturation between the rims and cores in the pulmonary arteries in the "experimental lobes."

Lack of Rims in Some of the Pulmonary Arteries of the "Experimental Lobes"

In the "experimental lobes" only 47% of the arteries had rims. This was no doubt due to inequalities in freezing time throughout the lobes as freezing took place. Vessels near the surface would be expected to freeze faster than vessels deeper in the lobe. Therefore only the deeper vessels froze slowly enough for rim formation to occur.

Statistics

Microspectrophotometer data from each experiment were processed by IBM 360 computer, which converted reflection ratios from the lungs to oxyhemoglobin saturation values by means of reverse linear regression based on the calibration data. Bonferroni multiple inference t tests (4) were applied to the mean saturation values in: pulmonary arteries and veins in the "control lobes;" arterial rims and cores, and veins in the "experimental lobes." Saturation differences were considered significant ($p<.05$) based on the results of this analysis.

Chapter 5 CALCULATION OF RIM THICKNESS: DIFFUSION + ADVANCING FRONT

In the cat experiments the size of the rims of oxygenated blood surrounding the mixed venous cores in the pulmonary arteries was the result of the conditions of low temperature and long freezing time that existed when the lungs were frozen. These conditions are not representative of the conditions that normally exist in the living animal. I made several calculations to estimate the rim size and, therefore, the fraction of oxygenated blood in pulmonary arterioles under normal conditions.

Assumptions

Figure 5-1 is a cross sectional diagram of a pulmonary arteriole where a rim of oxygenated blood is advancing from the wall of the vessel toward the deoxygenated core. Oxygenation occurs only at the interface between rim and core in this theory. Increasing rim thickness is assumed to be the result of two simultaneous processes: 1. diffusion of oxygen across the vessel wall, and through the oxygenated rim to the interface (Diffusion); and 2. movement of the interface toward the vessel core as a result of the diffusing oxygen having combined with hemoglobin at the interface (Advancing Front).

UMI

Figure 5-1

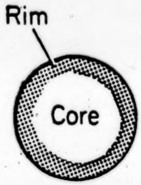

Cross-sectional view of a rim of oxygenated blood advancing inward from the vessel wall toward a core of deoxygenated blood.

Advancing Front Equation

$$F = \frac{H(D_{O_2} \cdot C \cdot T)^{1/2}}{(Hb)^{1/2}} \qquad \text{Eq. 5-1}$$

F	Distance front advances, cm
H	Proportionality factor, a function of $C/(Hb)$
C	Concentration of dissolved oxygen, ml/ml
T	Time, sec
D_{O_2}	Diffusion coeff. O_2 in plasma, 1.87×10^{-5} cm^2/sec
(Hb)	Hemoglobin concentration, g/dl

Roughton's Advancing Front Equation (28) (Equation 5-1) is assumed to describe the motion of the front from the vessel wall inward. The rate of diffusion of oxygen through the vessel wall depends on the diffusing capacity of the wall, and the oxygen partial pressure difference between alveolar gas and mixed venous (pulmonary arterial) blood. The diffusing capacities used are those of Sackner, et al(29)(Table 5-1).

The total time available for both processes to occur equals the transit time of the blood along a vessel of discrete diameter. Sackner's data are used (Table 5-1).

Cylindrical co-ordinates are not used. The oxygenation process is treated as if the blood were arranged in a plane sheet because the advance of the front will be small in the time available. The rim that is calculated to form is expressed as a percent of the vessel's cross sectional area.

The oxygenation process is assumed to be cumulative down the pulmonary arterial tree. Oxygenation that takes place in a vessel of any discrete diameter is added to that which occurred in larger vessels before arrival there. Assuming stream line flow, rims and cores do not mix. The percentage of blood that is oxygenated in the preceeding vessel determines the existing rim size when that blood enters the next successive vascular generation.

UMI

OXYGEN DIFFUSING CAPACITY OF PULMONARY ARTERIAL WALLS

VESSEL DIAM. µM	TOTAL BLOOD VOLUME ML	TRANSIT* TIME SEC	WALL DIFFUSING CAPACITY ML STPD/MIN X TORR
14	0.37	0.018	2.8×10^{-1}
30	0.15	0.0074	2.5×10^{-2}
50	0.12	0.0058	6.5×10^{-3}
70	0.11	0.0055	2.7×10^{-3}
90	0.10	0.0052	1.9×10^{-3}

* MODELED AFTER A 7 KG. DOG WITH PULMONARY BLOOD FLOW = 1.2 L/MIN

FROM: SACKNER, ET AL, (28)

TABLE 5-1

UMI

Results

Pertinent data to solve both the diffusion and advancing front equations were put into a small programmable calculator. The machine was programmed to solve both equations simultaneously, devoting different fractions of the total time available to each process. The calculation began with 99% of the available time devoted to advancement of the front. The remaining time was devoted to diffusion through the wall. The amount of oxygen required for the rim that was calculated to form was compared to that available through diffusion. The time fractions were incremented and the calculations repeated until the amount of oxygen required for the rim exactly equaled that available by diffusion through the wall. Diffusion though the wall was the limiting factor.

The results of the calculations are shown in Figure 5-2. Calculations were done for 3 different oxygen diffusion gradients. The pulmonary capillaries were assumed to have a diameter of 8 µm. Since we are considering only precapillary oxygenation, the data were plotted for vessels with diameters down to but not including 8 µm.

The points at which the plots terminate at the left are the predicted values of total precapillary oxygenation of mixed venous blood upon its arrival at the alveolar capillaries. The graph shows that under normal conditions at rest,(alveolar oxygen partial pressure = 100 torr, mixed venous oxygen partial pressure = 60 torr) mixed

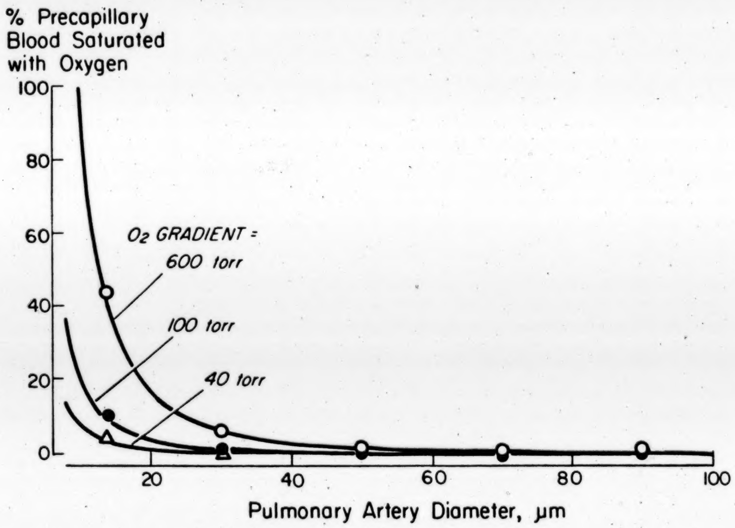

PERCENT PULMONARY PRECAPILLARY BLOOD SATURATED WITH OXYGEN AS A FUNCTION OF PULMONARY ARTERY DIAMETER AT 3 DIFFERENT OXYGEN DIFFUSION GRADIENTS

FIGURE 5-2

venous blood may be as much as 15% oxygenated upon reaching the capillaries. If the oxygen pressure difference between mixed venous blood and alveolar gas = 600 torr, as might be the case after a few breaths of 100% oxygen, the blood may be as much as 100% oxygenated before arrival at the capillaries.

POLYETHYLENE TUBE EXPERIMENTS

The technique for calculating the fraction of mixed venous blood oxygenated in precapillary lung vessels, described in the preceding paragraphs, is dependent on several reasonable assumptions. I checked their validity by constructing a polyethylene tube model that simulated the conditions that exist in the lung normally. I compared the observed results of the model experiments with the calculated results obtained using the same calculation techniques described above.

Experimental Conditions

I prepared three 100 or 200 cm lengths of polyethylene tubing (i.d. = 32 mm, wall thickness = 0.25 mm (P.E. 205)) and arranged them in coils. The coils were positioned vertically and wrapped with plastic bags. Humidified 95% oxygen/5% carbon dioxide was continuously flushed through the bags. A reservoir containing sheep blood that had been previously deoxygenated by equilibration with 95% nitrogen/5% carbon dioxide was positioned so that the blood flowed slowly through

UMI

the polyethylene coils. A stop watch and graduated cylinder were used to measure the flow.

After steady state conditions were established, both ends of the coils were stoppered, quickly removed from the plastic bags, and plunged into liquid propane (-170 C.). The frozen coils were placed in the cryostat and cut so that twenty 1 cm sections were taken from evenly spaced intervals along the coil's entire length. The twenty cross-sections were examined with the microspectrophotometer where rim widths, and rim and core reflection ratios were measured. The reflection ratios were not converted to oxyhemoglobin saturation values, but the ratios were consistent with oxyhemoglobin in the rims, and hemoglobin in the cores.

Results

The rim size in each length was plotted against the time the blood spent in the tube before reaching the point where that rim was located (Figure 5-3).

The Diffusion + Advancing Front Calculations were done for the conditions that existed for the blood when flowing through the coiled tubes. The permeability of the polyethylene tube wall to oxygen was assumed to be 6.9×10^{-10} ml/cm/cm^2/sec/cm Hg (26). The results of these calculations are also shown in Figure 5-3.

UMI

ACTUAL AND PREDICTED RATES OF RIM FORMATION IN POLYETHYLENE TUBES PERFUSED WITH DEOXYGENATED BLOOD

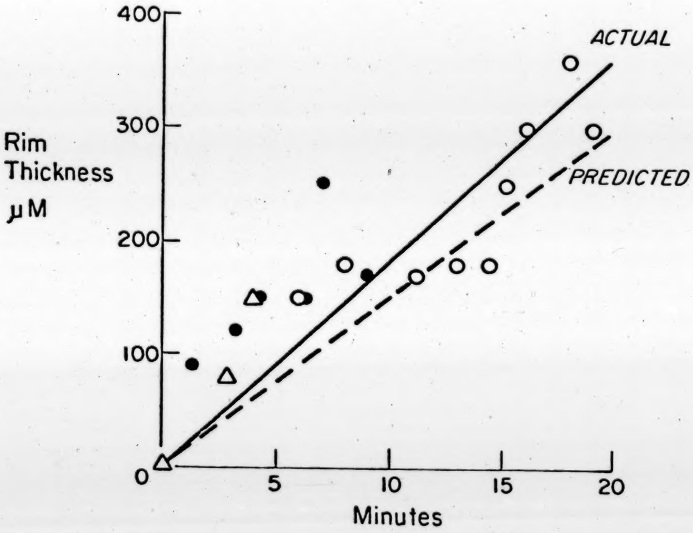

(EACH TYPE OF SYMBOL REPRESENTS ONE EXPERIMENT.)

FIGURE 5-3

DISCUSSION

In the polyethylene tube experiments, the oxygen diffusion gradient was made as large as possible at normal atmospheric pressure to overcome the diffusion resistance of the relatively thick polyethylene wall. The tubes still had to be very long, and the flow rates low for the blood to spend sufficient time in the tube for rim formation to occur. The low flows may have caused some of the red cells to settle out of suspension. This is one possible explanation for the scatter in the data in Figure 5-3.

There was always some delay in removing the coils from the plastic bag enclosures before plunging them into liquid propane. Thus the total time for diffusion at all points along the tubes was slightly greater than the data indicate. This influenced the results by increasing the rim size by a small but constant value at each point. The least squares regression plot was constrained to pass through the origin, but a least squares plot without that constraint would have a Y axis intercept value of about 60 µm, consistent with the results that a delay in freezing of a few minutes would cause.

Despite these slight deviations, there is good agreement between the observed results and those predicted. This clearly shows that the Diffusion + Advancing Front method of calculation is a reasonable way to predict the amount of oxygenation that is likely to occur in blood flowing through large vessels. This increases our confidence in using this technique to predict the amount of precapillary oxygenation that occurs in normal lungs.

The results of the calculations predict that mixed venous blood can receive significant amounts of oxygen before arriving at the alveolar capillaries.

UMI

Chapter 6 GENERAL DISCUSSION and CONCLUSIONS

Microspectrophotometry

The reflection microspectrophotometer I built is a convenient and reliable instrument for measuring oxyhemoglobin saturations in small frozen blood vessels. It records from an area 100 µm in diameter and does so with an accuracy of ± 5%.

While ice crystal scattering may have an important role in the theoretical foundation of this technique, it does not affect the method by which I make these measurements. I use frozen-blood calibration standards of known oxyhemoglobin saturation, and compare readings from experimental samples with those from the standards. Since light scattering affects both samples and standards identically, oxyhemoglobin saturation measurements need not be corrected for this property.

Several modifications are planned for the instrument to improve its performance. My goal is to record from smaller spots (30 µm or less) without increasing the illumination, thus avoiding the possibility of melting the specimen. I plan to do this by replacing the objective lens and the photomultiplier tubes with more sensitive equipment. A reflecting objective with twice the magnification of the present one has been ordered, as have two new photomultiplier tubes with 250X greater light sensitivity. The improved tube sensitivity

UMI

theoretically means that the same signal strength can be obtained from a spot only 6 μm in diameter without any increase in illumination.

Reflection readings from vessels as small as 6 μm would be complicated by the requirement that the specimen be at least 400 μm thick. Therefore an alternative technique is to utilize light transmitted through a specimen of precise thickness. All aspects of the present measuring system could be retained except that measurements would be made from light transmitted through the specimen and not from light reflected from it. In such a system the calibration standards and the specimens would be required to have identical thicknesses, but a reliable microtome could easily provide this reproducibility.

A desirable modification for the future would include replacement of the current white-light illumination system with the specific wavelength coherent light available from a laser. A single tunable dye laser is available that emits at selected peaks in the reflection spectra of hemoglobin and oxyhemoglobin. Use of this device would eliminate the needless spectral radiation of white light that impinges on the specimen, and would also reduce the total time the specimen is illuminated. Both factors would considerably reduce the chances of melting the specimen. Because the response time of the photomultiplier tubes is less than 5 nsec, the specimen would require illumination only for this period.

UMI

Laser light would also obviate the need for the interference filters that I now use for wavelength specificity. The present filters have half-intensity bandwidths of about 12 nm and transmit only 55% of the light they receive. Laser light has total bandwidths of 0.05 nm and suffers no loss of energy due to filtering.

Cat Experiments

The frozen cat lung experiments prove that precapillary oxygenation of mixed venous, pulmonary arterial blood can occur under favorable conditions. Several conditions are required: adequate oxygen diffusion pressure; blood vessel walls that are sufficiently permeable to oxygen; and sufficient time spent by the blood in these vessels for oxygenation to occur.

The freezing times in the experiments are long enough so that the oxygen partial pressure differences between mixed venous blood and the oxygen-filled alveoli are sufficient for oxygenation to occur through the walls of large pulmonary arteries. I measure such rim formation in vessels with diameters ranging from 3 mm to 0.5 mm, though it occurs first in the smallest arterioles where the walls are thin relative to blood volume. Staub's original observations in fact were made in vessels 100-200 μm in diameter (33) but the recording capabilities of my microspectrophotometer prevent me from recording from vessels smaller than 500 μm.

The time dependence of this phenomenon is illustrated by the results of the clamped hilum experiments. Clamping the hilar vessels at the moment of freezing stops blood flow and leaves stagnant pulmonary arterial blood in contact with alveolar oxygen long enough for the blood to become completely oxygenated before freezing is complete. All the frozen precapillary vessels were filled with fully oxygenated blood.

Oxygen pressure dependence is illustrated by experiments C 6 and C 7. When the lungs are ventilated with air the rims that form are significantly smaller than those in the experiments where 100% oxygen is used. In fact, the rims are reduced by approximately the ratio of the oxygen partial pressure difference.

Rims were not formed in all the arteries of the oxygen ventilated lobes. This is undoubtedly due to uneven advance of the freezing front while the lobes are being flooded with liquid propane. Though the propane is chilled to -170 C., alveolar gas insulates the lung against rapid heat loss and causes the freezing front to advance slowly. The propane is poured over the lobes from the top, so the bottom (dorsal) parts should freeze last. This results in the vessels near the top having the shortest period of exposure to oxygen before being frozen solid, while the vessels near the bottom are exposed longer and are therefore expected to have the largest rims. This is a simplified explanation of what actually occurs because the complex shape of the lobes makes it difficult to be precise about how the freezing front advances. It is therefore not possible to correlate rim size with the location of the rim-containing vessels within the lobe.

Models

The data of Sackner, et al (29) are used to calculate the amount of oxygenation that is expected to occur in the lung normally. These calculations lead to the conclusion that significant oxygenation may occur in precapillary arterioles. Sackner claims to have made similar calculations with his data, but came to the conclusion that no significant oxygenation occurs at the precapillary level, even when breathing 100% oxygen. The details of his calculations are not presented in his report. (Personal communication with him during a recent visit to San Francisco provided no further information. He had completed the experiments too long ago to recall the calculation techniques.)

My results are at odds with his conclusion. The vascular wall oxygen permeabilities and the calculated times of transit for the blood through these vessels indicate that significant oxygenation can occur based on the calculations I completed. The polyethylene tube experiments corroborate my method of calculation and show that it reasonably predicts the extent to which rim formation occurs.

UMI

Implications of the Results

Demonstration that oxygen crosses the walls of vessels larger than capillaries suggests that some modification may be required for the classical idea that gas exchange is confined to capillaries. Such modifications need not necessarily be extensive, for it is unlikely that this process is the major route of gas exchange in any except unusual circumstances. The diffusing capacities of the capillary walls far exceed those of the larger vessels. In addition, red blood cells spend over 100X more time in the anatomic capillaries than they do in arteries or arterioles of any discrete diameter. Thus the structure, arrangement, and distribution of the capillaries clearly implicate their role in the processes of gas exchange.

Still, precapillary exchange may not be insignificant. People in whom large quantities of alveolar capillary bed have been destroyed by diseases such as emphysema may obtain significant arterialization of their venous blood by this process especially when they are breathing 100% oxygen. Large pulmonary arterioles often cross the cavities this disease produces and blood flow through these vessels may be slow enough for the alveolar gas in the cavities to diffuse across the vessel walls and partially oxygenate the blood within. This suggests that so-called anatomic shunt calculated while breathing 100% oxygen may underestimate the shunt while breathing room air.

UMI

Duling and Berne (8) have suggested that significant oxygenation of peripheral tissue may occur as a result of oxygen diffusing out of the arterial blood through the walls of systemic arterioles. They used microelectrodes to measure the periarteriolar oxygen tensions in hamster cheek pouches and found longitudinal gradients of over 100 torr from the surface of vessels 80 um in diameter to the surfaces of the terminal arterioles in animals ventilated with 95% oxygen. Animals ventilated with air had gradients of over 20 torr (42 to 21 torr). Capillary oxygen partial pressures were always less than 5 torr below the values of the terminal arterioles.

The vast majority of tissue oxygenation in their experiments occurred as a result of precapillary oxygen diffusion. Blood flow rates were not quoted, but it is possible they were low in the conditions of their experiments. This would have provided long periods for diffusion through precapillary vessel walls and would explain the apparent low exchange rate in the capillaries.

These results suggest that precapillary gas exchange may be the major route of oxygen transfer from arterial blood to tissue in conditions when the larger gas transfer capacities of the capillaries are not required. Resting tissues, or tissues provided with low blood flows because of temporary diversions of blood to more metabolically active areas may obtain much of their oxygen directly from arterial blood flowing through arterioles. Certainly the oxygen needs of vascular smooth muscle may be entirely satisfied by oxygen diffusing from the lumen.

These results and the results of my own studies clearly indicate that oxygen is present within the walls of arterioles. This contributes further evidence to the role of oxygen in the local control of blood flow.

Hauge (13) completed several experiments with isolated rat lungs in which he tried to determine whether pulmonary arterial or alveolar hypoxia had the greater influence on the increases in pulmonary vascular resistance that occur during hypoxia. He found that pulmonary arterial hypoxemia without alveolar hypoxia produced no vasoconstrictor response, yet the pressor response to alveolar hypoxia could be diminished by increasing pulmonary arterial oxygen partial pressure above 120 torr. This implies that alveolar hypoxia has the greater overall influence on the increase in pulmonary vascular resistance, but shows that both factors determine the net response. This also shows that pulmonary vascular responses to hypoxia can be the result of cause-effect relationships within the lung without extrapulmonary nervous intervention. Pulmonary blood flow can be controlled locally. There is much disagreement about how this control is mediated: whether through the release of vasoactive substances from secretory cells, or as a result of the direct action of decreased oxygen tension on pulmonary vascular smooth muscle. In either case the response must be due to the presence of oxygen in the pulmonary vascular wall. My work clearly shows that oxygen is present there.

CONCLUSIONS

My work shows that significant oxygenation of mixed venous pulmonary arterial blood can take place before its arrival at the alveolar capillaries. The data of Sackner, et al (29) used to estimate the extent of this process are imprecise because of the methods they used to obtain them. This may therefore result in considerable debate about how extensive this process is. It does not however alter the basic conclusion that precapillary oxygenation occurs.

The location of the pulmonary arterial system within the oxygen-rich lung parenchyma, combined with the exponential increase in diffusing capacities of its vessel walls along the vascular tree make this a logical and reasonable conclusion.

UMI

REFERENCES

1. Amy,L.: Sur La Courleur Des Corps Par Reflexion, Revue D'Optique, 16(3): 81-92, 1937.

2. Anderson, N., N. Staub, J. Hoffman, et al: Determination of Oxyhemoglobin Saturation in Frozen Blood by Reflection Microspectrophotometry, unpublished manuscript, 1971.

3. Brinkman, R., W. Zylstra: Determination and Continuous Registration of the Percentage Oxygen Saturation in Clinical Conditions, Archivum Chirurgicum Neerlandicum, 1: 177-183, 1949.

4. Cohen, J., P. Cohen: Applied Multiple Regression p. 157, Wiley and Sons, N.Y., 1975.

5. Crank, J.: The Mathematics of Diffusion 2nd ed. p. 327, Clarendon Press, Oxford, 1975.

6. Drabkin, D., J. Austin: A Technique for the Analysis of Undiluted Blood and Concentrated Hemoglobin Solutions Journal of Biological Chemistry, 112: 105-115, 1935-36.

7. Drabkin, D., C. Schmidt: Observation of Circulating Blood in vivo, and the Direct Determination of Hemoglobin in Arterial Blood, Journal of Biological Chemistry, 157: 69-83, 1945.

8. Duling, B., R. Berne: Longitudinal Gradients in Periarteriolar Oxygen Tension, Circulation Research, 27: 669-678, 1970.

9. Enson, Y., W. Briscoe, M. Polanyi, et al: In vivo Studies with an Intravascular and Intracardiac Reflection Oximeter, Journal of Applied Physiology, 17(3): 552-558, 1962.

10. Feisal, K., J. Soni, A. DuBois: Pulmonary Arterial Circulation Time, Pulmonary Arterial Blood Volume, and the Ratio of Gas to Tissue Volume in the Lungs of Dogs, Journal of Clinical Investigation, 41(2): 390-400, 1962.

11. Gamble, W., C. LaFarge, D. Fyler, et al: Regional Coronary Venous Oxygen Saturation and Myocardial Oxygen Tension Following Abrupt Changes in Ventricular Pressure in the Isolated Dog Heart, Circulation Research, 34: 672-681, 1974.

UMI

12. Gordy, E., D. Drabkin: Determination of the Oxygen Saturation of Blood by a Simplified Technique, Applicable to Standard Equipment, Journal of Biological Chemistry, 227(1): 285-299, 1957.

13. Hauge, A.: Hypoxia and Pulmonary Vascular Resistance. The Relative Effects of Pulmonary Arterial and Alveolar Oxygen Pressure, Acta Physiologica Scandinavica, 76: 121-130, 1969.

14. von Hayek, H., The Human Lung, p. 243, Hafner, N.Y., 1960.

15. Jameson, A.: Diffusion of Gases from Alveolus to Precapillary Arteries, Science, 139: 826-828, 1963.

16. Kato, M., N. Staub: Response of Small Pulmonary Arteries to Unilobar Hypoxia and Hypercapnia, Circulation Research, 19: 426-440, 1966.

17. Keilin, D., E. Hartree: Effect of Low Temperature on the Absorption Spectra of Haemoproteins; With Observation on the Absorption Spectrum of Oxygen, Nature, 164: 254-259, 1949.

18. Klingenmaier, C., M. Behar, T. Smith: Blood Oxygen Content Measured by Oxygen Tension after Release by Carbon Monoxide, Journal of Applied Physiology, 26(5): 653-655, 1969.

19. Marx, T., W. Snyder, A. StJohn, et al: Diffusion of Oxygen into a Film of Whole Blood, Journal of Applied Physiology, 15(6): 1123-1129, 1960.

20. Millikan, G.: The Oximeter, an Instrument for Measuring Continuously the Oxygen Saturation of Arterial Blood in Man, Revue of Scientific Instruments, 13: 434-444, 1942.

21. Mook, G., O. van Assendelft, W. Zijlstra: Wavelength Dependency of the Spectrophotometric Determination of Blood Oxygen Saturation, Clinica Chimica Acta, 26: 170-173, 1969.

22. Munson, E., W. Paul, J Perry, et al: Early Detection of Venous Air Embolism Using a Swan-Ganz Catheter, Anesthesiology, 42(2): 223-226, 1975.

23. Munson, E.: Effect of Nitrous Oxide on the Pulmonary Circulation During Venous Air Embolism, Anesthesia and Analgesia, 50(5): 785-792, 1971.

UMI

24. Pittman, R., B. Duling: A New Method for the Measurement of Percent Oxyhemoglobin, Journal of Applied Physiology, 38(2): 315-320, 1975.

25. Pittman, R., B. Duling: Measurement of Percent Oxyhemoglobin in the Microvascular, Journal of Applied Physiology, 38(2): 321-327, 1975.

26. Raff, R., K. Doak (eds.): Crystalline Olefin Polymers part 2, p. 147, Interscience Publishers (J. Wiley and Sons), N.Y., 1964.

27. Roughton, F.: Diffusion and Simultaneous Chemical Reaction Velocity in Haemoglobin Solutions and Red Cell Suspensions, Progress in Biophysics and Biophysical Chemistry, 9: 55-106, 1959.

28. Roughton, F., R. Forster: Relative Importance of Diffusion and Chemical Reaction Rates in Determining Rate of Exchange of Gases in the Human Lung, with Special Reference to True Diffusing Capacity of Pulmonary Membranes and Volume of Blood in the Lung Capillaries, Journal of Applied Physiology, 11: 290-302, 1957.

29. Sackner, M., K. Feisal, D. Karsch: Size of Gas Exchange Vessels in the Lung, Journal of Clinical Investigation, 43(9): 1847-1855, 1964.

30. Scheffé, H.: A Statistical Theory of Calibration, The Annals of Statistics, 1(1): 1-37, 1973.

31. Sinha, A., J. Neubauer, J. Lipp: Oxygen Saturation Determination in Frozen Blood, Microvascular Research, 10(3): 312-321, 1975.

32. Sobol, B., G. Bottex, C. Emirgil, et al: Gaseous Diffusion from Alveoli to Pulmonary Vessels of Considerable Size, Circulation Research, 13: 71-79, 1963.

33. Staub, N.: Gas Exchange Vessels in the Cat Lung, Federation Proceedings, 20: 107, 1961 (abstract).

34. Staub, N.: Alveolar-Arterial Oxygen Tension Gradient Due to Diffusion, Journal of Applied Physiology, 18(4): 673-680, 1963.

UMI

35. Staub, N.: The Sensing of Oxygen Tension in the Pulmonary Circulation, Advances in Experimental Biology and Medicine, 78: 151-162, 1977.

36. Staub, N., W. Storey: Relation Between Morphological and Physiological Events in Lung Studied by Rapid Freezing, Journal of Applied Physiology, 17(3): 381-390, 1962.

37. Vreim, C., N. Staub: Indirect and Direct Pulmonary Capillary Blood Volume in Anesthetized Open-Thorax Cats, Journal of Applied Physiology, 34(4): 452-459, 1973.